

**6th US-Russian Pu Science Workshop
Lawrence Livermore National Laboratory
University of California, Livermore, California
July 14 and 15, 2006**

Local Chairs:

**Michael Fluss, James Tobin, Adam Schwartz
LLNL, Livermore, USA**

**Alexander V. Petrovtsev,
RFNC • VNIITF, Snezhinsk, Russia**

**Boris A. Nadykto,
RFNC • VNIIEF, Sarov, Russia**

**Lidia F. Timofeeva,
VNIINM, Moscow, Russia**

**Siegfried S. Hecker, (Luis Morales POC)
LANL, Los Alamos, USA**

**Valentin E. Arkhipov,
IMP, Ural Branch of RAS, Yekaterinburg, Russia**

**This is a satellite meeting of the
“Pu Futures—The Science 2006 International Conference”,
9-13 July 2006, Asilomar Conference, Grounds, Pacific Grove Ca.**

**The workshop is hosted by LLNL, under the aegis of the United
States/Russian Federation Scientific and Technical Collaboration pursuant
to the 2002 DOE-NNSA/NA-1 MinAtom (RosAtom) agreement.**

Russian-USA Pu Workshop, LLNL, Livermore, CA, USA-July 14-15, 2006

Friday, July 14

- 6:30 AM Breakfast starts at Residence Inn
- 7:00 AM First Bus from Residence Inn to West Gate Badge Office
- 7:15 AM Badging starts at WGBO
- 8:00 AM Arrival and Registration (Bldg 123 Area)
- 8:30 AM Workshop Welcome by K. Budil, L. Terminello, L. Morales and J. Tobin
- 8:45 AM **Oral Session One (Bldg 123 Auditorium):
Phase Stability, Phase Transformations, and Aging Effects**
Co-Chairs: Ted Massalski (CMU) and Boris Nadykto (VNIIEF)
- 8:45 AM **L. Timofeeva (VNIINM)**
"Interaction of Pu, Pu-Al and Pu-Ga Alloys with Radiogenic Elements"
- 9:15 AM **K. Blobaum (LLNL)**
"Delta/Alpha-Prime Phase Stability in Pu-Ga Alloys"
- 9:45 AM **A. Laushkin (VNIINM)**
"Structural Changes in β -phase Alloys Based on Pu²³⁹ and Pu²⁴² Under Self-Irradiation"
- 10:15 AM Break
- 10:30 AM **D. Harbur (LANL)**
"The Effect of Pressure on Phase Stability in the Pu-Ga Alloy System"
- 11:00 AM **I. Konovalov (VNIINM)**
"Computation of Irradiation Damage in Alpha-Decay Actinides"
- 11:30 AM Discussion Period
- 12:00 PM Lunch- Catered in B123 Area
- 12:00 PM **Poster Session and Microscopy Events**
Poster Presentations and Discussions (Bldg 123 Area)
Small group tours of the DTEM (Bldg 298)
Small Panel Discussion of LLNL Microscopy Capabilities (Bldg 123 Audit.)
Oral Presentation by K. Moore, "Transmission electron microscopy of actinide materials"
- 3:30 PM **Oral Session Two (Bldg 123 Auditorium):
Fundamental Physical Properties/Electronic Structure of Actinides**
Co-Chairs: Bill Wolfer (LLNL) and V. Anisimov (RAS-IMP)
- 3:30 PM **A. Kutepov (VNIITF)**
"Details of relativistic Hartree-Fock method as applied to crystals: Differences from density functional theory"
- 4:00 PM **P. Soderlind (LLNL)**
"Density Functional Calculations of β -Pu-Ga (Al) Alloys"
- 4:30 PM **M. Baskes (LANL)**
"LANL Computational Theory"
- 5:00 PM Break
- 5:15 PM **S. Verkhovskii (RAS-IMP)**
"Peculiar magnetic ordering in Pu_{0.95}Ga_{0.05} alloy at low temperature"
- 5:45 PM **B. Nadykto (VNIIEF)**
"Fine splitting of energy levels in many-electron atoms and ions"
- 6:15 PM Discussion Period
- 6:45 PM Workshop Banquet (West Cafeteria)
- 10:00 PM Transport to hotel

Russian-USA Pu Workshop, LLNL, Livermore, CA, USA-July 14-15, 2006

Saturday Morning, July 15

- 7:00 AM Breakfast starts at Residence Inn
7:30 AM First Bus from Residence Inn to B123
8:00 AM Arrival and Registration (Bldg 123 Area)
8:15 AM **Oral Session Three (Bldg 123 Auditorium):
Dynamics of Aged Materials: Experiment, Theory and Simulations**
Co-Chairs: J. Moriarty (LLNL) and E. Kozlov (VNIITF)
- 8:15 AM **K. Budil (LLNL)**
"Dynamic Material Properties Experiments at LLNL"
- 8:45 AM **E. Kozlov (VNIITF)**
"Explosive experiments for studying dynamic properties of transition metals, some actinides and alloys on their basis"
- 9:15 AM **R. Hixson (LANL)**
"Overview of some dynamical material properties research; continuum level to microscopic level"
- 9:45 AM Break
- 10:00AM **B. Uchaev (VNIIEF)**
"On the possibility of application of ultrashort pulses of laser radiation to study the properties of metallic plutonium under extreme conditions"
- 10:30AM **L. Egorov (VNIIEF)**
"X-ray diffraction studies of the relaxation process of dynamically compressed crystals"
- 11:00AM **Workshop Discussion and Summary-**
S. Hecker, M. Fluss, B. Nadykto, L. Timofeeva
- 12:00PM Lunch- Catered in B123 Area, Discussion of Workshop
1:00 PM Transport to Hotel

Friday July 14, 12:00PM Poster Session

VNIINM (Bochvar) Posters

- A. Karnozov "A new method of describing uranium oxidation in water vapor"
L. Timofeeva "Phase Transformations in Pu-Al and Pu-Ga Alloys. Effects of Pressure and Temperature on the Kinetics of the Delta-Phase Decomposition"
A. Udovsky "The Application of Thermodynamic Approach for Development of chemically stable soft X-Ray Multilayer Mirrors Based on depleted Uranium"

VNIIEF (Sarov) Posters

- B. Nadykto "Instability of actinide electron structure under high pressure"
A. Postnikov "SHS method for immobilization of plutonium containing waste"
V. Pushkov "Experiments and model of dynamic deformation of uranium-238 and its alloy with Mo"

VNIITF (Snezhinsk) Posters

- E. Clementyev "On the feasibility of inelastic neutron scattering experiments on Pu-239 based materials"
V. Dremov "Monte Carlo and Molecular Dynamics simulation of radiation damage evolution and Helium dynamics in Pu"

Russian-USA Pu Workshop, LLNL, Livermore, CA, USA-July 14-15, 2006

- V. Elkin "Applicability of Elastic-Plastic Estimations to the Energy of Mixing of Solid Solutions"
- A. Mirmelstein "Enhancement of localized magnetism due to Kondo-ions"
- A. Troshev "Influence of decay-induced internal stresses on beta-phase nucleation during alpha-beta transformation of unalloyed plutonium under isothermal condition"

RAS-IMP (Ekaterinburg) Posters

- V. Anisimov "The theory of electronic structure and magnetic properties of Pu and Pu alloys"
- M. Korotin "Influence of interstitial impurity and vacancy on α -Pu magnetic state: ab initio investigation"
- Y. Piskunov "Low frequency spin dynamics of f electrons probed by ^{69}Ga in $\text{Pu}_{0.095}\text{Ga}_{0.05}$ alloy"

LANL (Los Alamos) Posters

- M. Baskes "Phase-field modeling of Coring Structure Evolution and Ga Homogenization Kinetics in Pu-Ga Alloys"
- C. Cady "Structure/Property Relationships of U-6 wt.% Nb as a Function of Temperature, Strain Rate and Aging"
- E. Cerreta "The Characterization of Shear Deformation and Shock damage in U6Nb"
- N. Curro "PuCoGa5: Bridging the Gap between Heavy Fermion and High Temperature Superconductivity"
- A. Migliori "Temperature and time- dependence of the elastic moduli of Pu and Pu-Ga alloys"
- J. Mitchell "The α - β ' Transformation in Aged Pu-Ga Alloys"
- L. Morales "Aging and Phase Stability in Delta-Stabilized Pu: Local and Long-Range Order"
- J. Thompson "Superconductivity and Magnetism in PuCoGa5 and Related Materials"
- S. Valone "Multi-Scale Modeling of Aging in Pu Alloys"
- A. Zubelewicz "Factors Contributing to the Dynamic Behavior of Metals"

LLNL (Livermore) Posters

- E. Bringa "Molecular dynamics simulations of the interaction between shock waves and high-symmetry intergranular boundaries"
- B. Chung "Spectroscopic and Physical Measurements of Aging in Pu"
- A. Kubota "Dynamic Strength of Metals in Shock Deformation"
- S. McCall "Self-damage and Magnetic Susceptibility in Pu and Pu Alloys as a Probe of the 5f electrons"
- K. Moore "Oxidation and aging in U and Pu probed by spin-orbit sum rule analysis: Indications for covalent metal-oxide bonds"
- B. Remington "High Pressure, High Strain Rate Laser Materials Science"
- J. Tobin "Determining the Electronic Structure of Pu using Unorthodox Spectroscopies"
- M. Wall "Actinide Sample Preparation for Materials Science, Chemistry and Physics"
- C.S. Yoo "New opportunities for high-pressure materials research at the HPCAT at APS"

Friday, July 14, 2006

Oral Session One

Morning

Interaction of Pu and Pu-Ga Alloys with Radiogenic Elements

L.F. Timofeeva

A.A.Bochvar VNIINM (All-Russian Research Institute of Inorganic Materials), Moscow, Russia

In the context of accumulation of U, Np, Am impurities resulted from radioactive decay of Pu, interaction of these elements with Pu, Pu-Ga alloys is of interest.

Binary phase diagrams for Pu with uranium, neptunium, americium have similarity and some distinctions. These elements produce a wide regions of solid solutions based on ϵ -Pu (U, Np, Am), β -(Np, U), α -Pu (Np) and δ -Pu (Am), but do not form any intermetallic compound¹. Americium increases, and U and Np decrease plutonium' melting point and ϵ - and δ -phase formation temperatures. Accordingly, the character of distribution of these elements on a grain (or on a dendritic cell) at a nonequilibrium crystallization will be different. Americium concentration on the grain boundary is lower, and U and Np concentration is higher than in the grain center.

The absence of the compounds suggests that in the case of triangulation of ternary systems like Pu-Ga-(U, Np, Am), a side of binary Pu-(U, Np, Am) systems are not sliced by quasi-binary section lines.

Ternary phase diagrams for Pu-Ga with U, Np, Am were examined in the region of δ -solid solutions relying on present-day knowledge obtained for elements of different solubility in δ -phase. In δ Pu, the solubility of U is very low, that of Np at 400C is up to 3% but unstable at room temperature while Am forms a wide region of δ -solid solutions that are stable at room temperature. These three elements pertain to three different groups as shown in

Figure. 1, where three types of schematic binary phase diagrams connected on Pu axis², represent interaction of Pu-Ga alloys with elements of different solubility in δ - Pu phase.

These diagrams practically identical with flat unrolling Pu angle in the ternary Pu-Ga-(alloying element) phase diagrams, on the one hand which is binary Pu-Ga phase diagrams, on the other hand it is binary Pu-(U, Np, Am) phase diagrams.

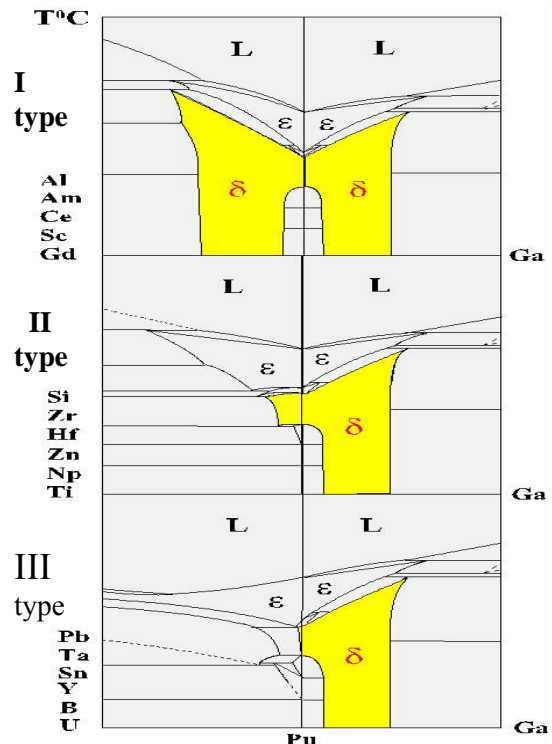


Fig 1: Three types of schematic binary phase diagrams connected on Pu axis: on the right Pu-Ga diagram, on the left Pu-(alloying element) diagrams

The relevant isothermal sections (see Figure 2) reflect their variations on cooling from 400 °C (δ -region) to room temperature.

Knowledge of the ternary diagram structure in the Pu region was supported by experimentally plotted isothermal sections of ternary systems yielding continuous solid solution areas (Pu-Ga-Al³, Pu-Al(Ga)-Ce) and limited solubility areas in δ -phase (Pu- Ga-Ti). Based on these data isothermal sections for the ternary (Pu- Ga) + (U, Np, Am) systems were plotted (see Figure 3).

As shown by the phase diagrams, U, Np, Am singly or in combination expand the two phase ($\alpha+\delta$) region in the ternary systems under consideration by displacing the δ -region boundary to higher compositions. Clearly this tendency can show up at a low content of accumulated radiogenic elements like U, Np, Am.

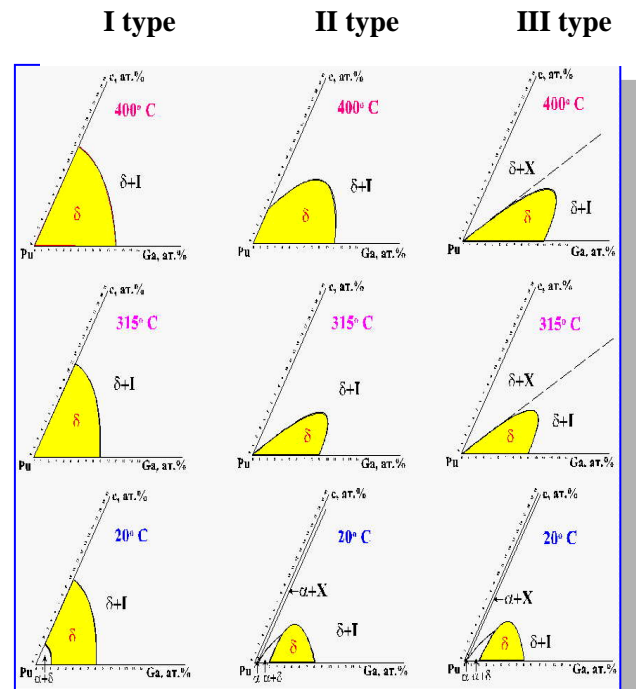


Fig 2: Schematic isothermal sections at 400, 315 and 20°C for the three types of phase diagrams Pu-Ga-(alloying element).

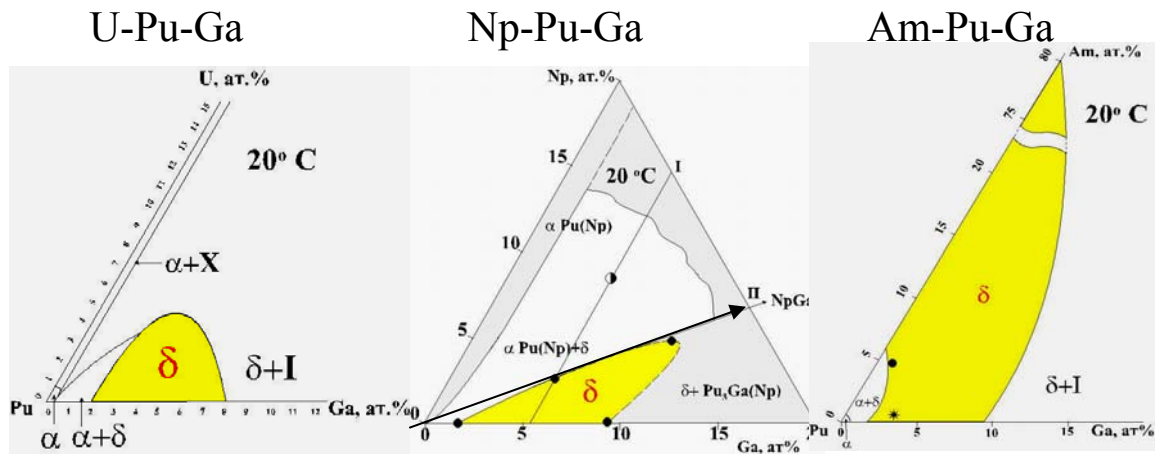


Fig 3: Isothermal sections at 20°C for the Pu angle of the ternary phase diagrams Pu-Ga with U, Np, Am

- 1 Binary Phase Diagrams. Ed. N.P.Lyakishev, 3 Vol., Moscow, Mashinotr., in Rus. (2000).
- 2 S.S. Hecker, LAS, **26**, c.292 (2000).
- 3 N.T.Chebotarev, E.S.Smotrinskaya, M.A.Andrianov, O.E.Kostyuk, Pu-75, Eds. H.Blunk and R.Lindner (1976).

Delta/Alpha-Prime Phase Stability in Pu-Ga Alloys

K.J.M. Blobaum, B. Oudot, M.A. Wall, A.J. Schwartz
Lawrence Livermore National Laboratory

In a Pu-2.0 at% Ga alloy, the ductile face-centered cubic δ phase can be retained in a metastable state at ambient conditions. Under these conditions, the thermodynamically stable phases are α (monoclinic) + Pu_3Ga ,^{1,2} but the complete eutectoid decomposition is estimated to take on the order of 10,000 years.² When the metastable δ phase is cooled to approximately -120°C , it partially transforms to the α' phase. The α' phase is monoclinic like the α phase, but it has Ga supersaturated in the lattice, which leads to slightly larger lattice parameters. The $\delta \rightarrow \alpha'$ martensitic phase transformation can occur with continuous cooling, or with sub-ambient isothermal holding.³⁻⁵ The isothermal $\delta \rightarrow \alpha'$ phase transformation is reported to have unusual double-C curve kinetics in some Pu-Ga alloys; this behavior is not well understood. Upon heating, the α' phase reverts to the δ phase via a burst martensite mode beginning at approximately 30°C .⁵ Here, we present and discuss these significant findings from our investigations of δ/α' phase stability in a Pu-2.0 at% Ga alloy.

During the $\alpha' \rightarrow \delta$ reversion, steps are observed in resistometry and dilatometry data and sharp spikes are seen in differential scanning calorimetry (DSC) data.⁵ In most materials, these three techniques show smooth variations corresponding to phase transformations. We attribute these unusual steps and spikes to transformation and reversion via a burst martensite mode. Because the densities of the δ and α' phases differ by 25%, plastic accommodation by the δ matrix must occur. When an α' particle reverts back to the δ phase, it leaves a residual stress field behind. Near the reverted α' particle's tips, the residual stresses accelerate additional α' reversion and along the length of the particle they retard it. Thus, additional α' particles near the tip of the reverted particle can immediately revert and a cascade of reversion is initiated. Each step (dilatometry and resistometry data) or spike (DSC data) corresponds to a cascade of α' reversion. The cascades are quenched by a combination of stress and temperature changes resulting from the reversion, which is endothermic and may cause local cooling in the sample.

Although it is reported in the literature that successive thermal cycling results in less α' transformation on each cycle,^{4,6} we have found that a sequence of high-temperature annealing followed by ambient-temperature "conditioning" prior to each thermal cycle results in the same amount of transformation in each cycle.⁷ For conditioning times between 0 and 6 hours, the amount of α' formed upon cooling increases with conditioning time. Additional conditioning, up to 70 hours, does not increase α' formation. During the ambient-temperature conditioning treatments, we hypothesize that embryos of the thermodynamically stable α phase form. Upon cooling, these embryos nucleate or form α' particles. Self-irradiation by the plutonium is likely to enhance diffusion and enable α embryo formation. A modeling approach based on classical nucleation theory is used to describe α embryo formation during the conditioning treatments.

Our preliminary results from investigations into the nature of the double-C curve kinetics of the isothermal $\delta \rightarrow \alpha'$ transformation suggest a confirmation of the time-temperature-transformation (TTT) curves published by Orme, *et al.*⁸ The TTT curves published by Orme, *et al.* investigate transformation behavior for isothermal holds of 110 minutes or less. Here, we

present data from a novel DSC technique that suggests the double-C curve kinetics persist during holds as long as 1080 minutes (18 hours).

This work was performed under the auspices of the U.S. Department of Energy by University of California Lawrence Livermore National Laboratory under contract No. W-7405-Eng-48.

References

1. N. T. Chebotarev, E. S. Smotriskaya, M. A. Andrianov, and O. E. Kostyuk: in *Plutonium 1975 and Other Actinides*, edited by H. Blank and R. Lindner, North Holland Publishing Co., Amsterdam, 1975, pp. 37-46.
2. S. S. Hecker and L. F. Timofeeva: *Los Alamos Science*, 2000, vol. 26, pp. 244-251.
3. J. T. Orme, M. E. Faiers, and B. J. Ward: in *Plutonium 1975 and Other Actinides*, edited by H. Blank and R. Lindner, North-Holland Publishing Company, Amsterdam, 1975, pp. 761-773.
4. S. S. Hecker, D. R. Harbur, and T. G. Zocco: *Prog. Mater. Sci.*, 2004, vol. 49, pp. 429-485.
5. K. J. M. Blobaum, C. R. Krenn, J. N. Mitchell, J. J. Haslam, M. A. Wall, T. B. Massalski, and A. J. Schwartz: *Metall. Mater. Trans. A*, 2006, vol. 37A, pp. 567-577.
6. J. N. Mitchell, M. Stan, D. S. Schwartz, and C. J. Boehlert: *Metall. Mater. Trans. A*, 2004, vol. 35A, pp. 2267-2278.
7. K. J. M. Blobaum, C. R. Krenn, M. A. Wall, T. B. Massalski, and A. J. Schwartz: *Acta mater.*, 2006.
8. B. J. P. Oudot, K. J. M. Blobaum, M. A. wall, and A. J. Schwartz: in *Actinides 2005--Basic Science, Applications and Technology*, edited by J. L. Sarrao, A. J. Schwartz, M. R. Antonio, P. C. Burns, R. G. Haire, and H. Nitsche, *Mater. Res. Soc. Symp. Proc.*, vol. 893, Warrendale, PA, 2006, pp. 0893-JJ05-02.

Structural Changes in δ -phase Alloys Based on Pu^{239} and Pu^{242} Under Self-Irradiation

V.K. Orlov, M.Yu. Bakursky, A.V.Laushkin, M.Yu.Polyakov, V.V.Sipin, V.P.Glazkov*, V.A.Somenkov*

All-Russian Research Institute of Inorganic Materials

*Russian Research Center Kurchatov Institute

An increase in the crystal lattice parameter of δ -phase alloys stored for a long period of time, or the aging of δ -Pu alloys as is most commonly said, has long been known and exhibited by a variety of compositions [1] (Fig.1). S.T.Konobeyevsky and N.T.Chebotarev [2] from VNIINM have long attributed the process to non-ideality of the compact fcc packing, resulted from displacement of atoms located in the faces of a crystal from their original positions.

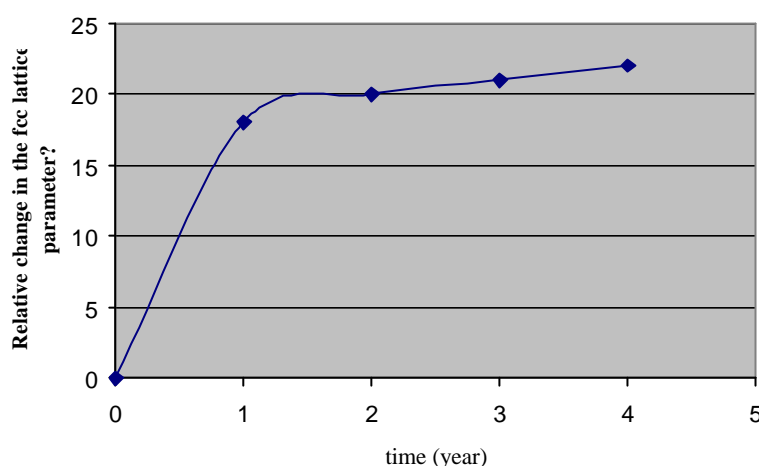


Fig.1 Relative change in the fcc lattice parameter ($\Delta a/a \cdot 10^4$) of solid solution in the Pu-18 at% Ga

A critical review [3] of this model shows that the displacements are bound to initiate super-structural reflections, which but they have not been detected yet by X-ray diffraction analysis.

A series of recent experiments caused a rebirth of interest in structural aging models. X-ray diffraction examination of aged δ -phase materials shows that a short-term laser heating with no surface melting restores the crystal lattice parameters to their original position. The melting freedom was surveyed as follows. The laser melting is indicated by capillary flow resulted from different viscosity and different surface tension energy of liquid areas containing an alloying element in different amount. The capillary flow results in agitation and a higher homogeneity.

Our latest experiments with aged alloys showed no laser-induced change in homogeneity but the aging effect was relieved, i.e. the crystal lattice parameter was replaced in its original position.

RRC KI analyzed the aging models by neutron diffraction using samples based on Pu^{242} and small amounts of Pu^{238} ; the presence of the latter increased the aging process about a four times. The high-temperature δ -structure was stabilized by gallium. The typical neutron diffraction pattern is given in Fig. 2.

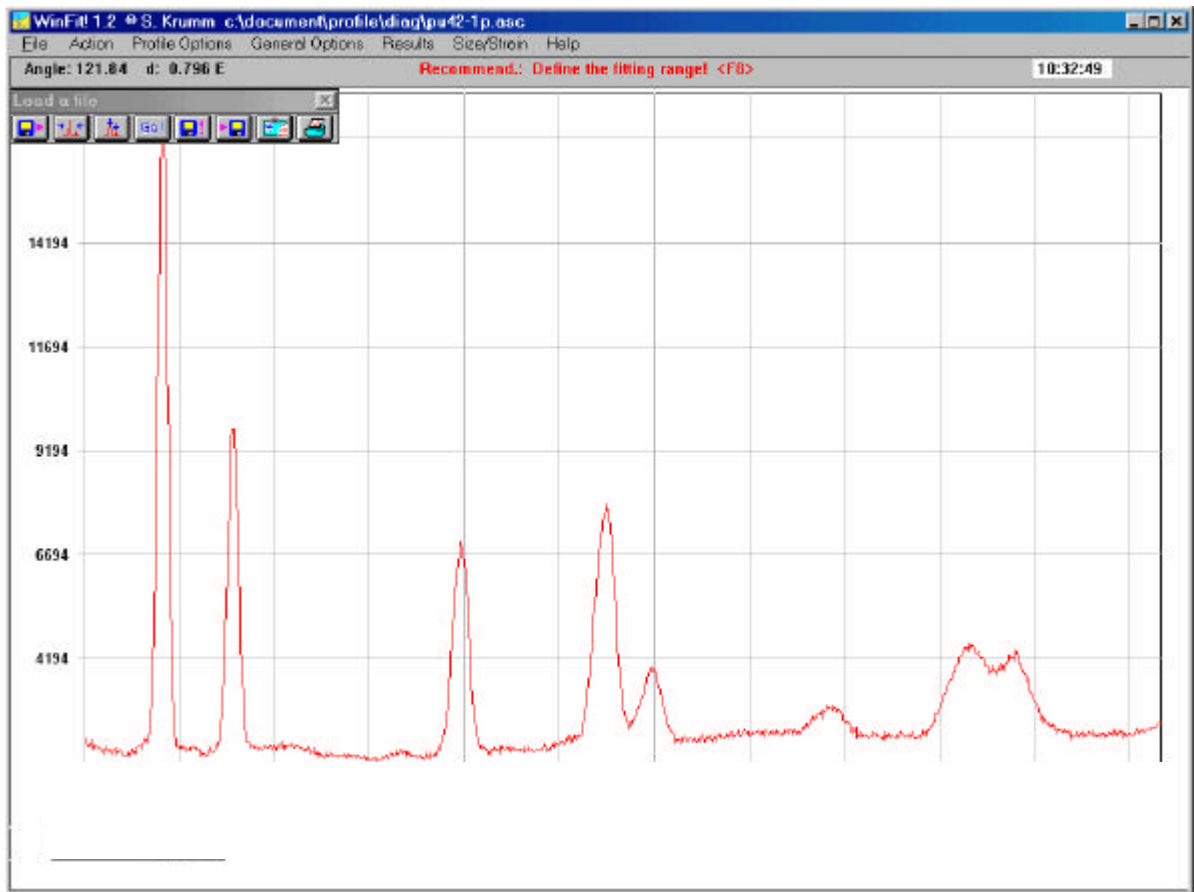


Fig 2 Neutron diffraction pattern for the Pu²⁴² -base alloy

Apart from the fcc structural reflections, the neutron diffraction pattern (Fig.2) shows faint but clear additional reflections the nature of which is still under research. Standard experiments showed that the latter reflections resulted from scattering by the samples rather than by the material of a container or a holder. The part of the widest reflections can be classified in terms of doubled lattice parameters but as well it can be explained both by atom displacement and by the reflections from radiation with a wave length of $\lambda/2$. However the part of the narrowest reflections cannot be explained in such a manner.

Fig. 3 shows the integral width of the structural reflections as a function of a scattering angle for the initial sample and this sample after aging. The observed higher non-monotony of variation in the integral width of reflection with increasing scattering angle can be assigned to a change in internal micro-stresses.

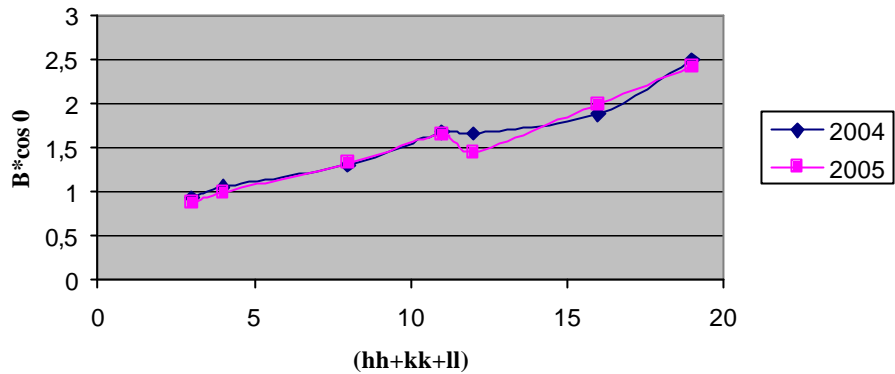


Fig.3. Reflection width as a function of a scattering angle and aging period

In parallel with the structural investigation, the Debye-Waller factor (DVF) was determined at various aging stages.

The data obtained indicate a number of different aging stages resulted from possible structural rearrangement, variations in force constants and the generation of defects due to self-irradiation. In any case the behavior of the alloy is different in short-term and long-term storage. This difference will be the subject of further investigation.

1. N.?. Chebotarev, ? .? .? ndrianov, L.F. Timofeyeva «Effect of Long-Term Self-Irradiation at Room Trmperature on the Structure of Pu₃Ga and Diffuse δ + Pu₃Ga Alloys» Problems of Nuclear Science and Technology Nuclear Science of Materials. v. 4 (15) p. 40
2. N.?. Chebotarev, S.T. Konobeyevsky «On the Structure and Thermal Expansion of δ- and δ'- Pu». Atomic Power v.10, # 1, 1961.
3. J. Marpls, J. Lee «On the Structure of δ - Pu». Atomic Power. May 1962. p. 423

The sanction to an information exchange dd-658

The Effect Of Pressure On Phase Stability In The Pu-Ga Alloy System

D.R. Harbur

Los Alamos National Laboratory, Los Alamos NM 87544 USA

Abstract

In examining and analyzing over three decades of research on the transformations involved in the Pu-Ga alloy system, it has become evident that the data is comprised of many seeming incongruities and contradictions. Plutonium is not the easiest material to generate data on, and because of the complexities in its phase relationships, and its sensitivities to alloying, temperature and pressure, the analysis of the data is not always straightforward. The best technique that the metallurgy community has for identifying the different phases in Pu is x-ray diffraction, and many capable scientists have well developed the art as it is applied to Pu and its alloys. X-ray diffraction, however, is not a very good tool for studying non-diffracting disordered materials. In this paper we have shown that under certain processing methods large amounts of a non-diffracting disordered-state are formed in Pu-Ga alloys, which we call the amorphous-state. The amorphous-state is certainly not an equilibrium-state, but it nevertheless can be formed under certain pressure-states, and more surprisingly once formed can persist for extended times and temperatures at ambient pressures. Being a physical-state, the amorphous-state has distinct physical properties, meta-stability and sensitivities to Ga content.

When Pu is alloyed with small amounts of Ga and homogenized, the δ -phase can be stabilized over a reasonable temperature and pressure range. At low temperatures, the δ -phase will begin to transform to the α' -phase, with the transformation temperature being dependent upon the amount of Ga. At very low Ga contents near 1 at. % Ga the δ -phase will begin to transform very near room temperature and the transformation products are a mixture of the α' -phase and the amorphous-state. At 0.68 at. % Ga all of the δ -phase transforms into the α' -phase and the amorphous-state upon cooling to room temperature.

The δ -phase also becomes unstable at high hydrostatic-pressures, and this instability is also strongly related to the Ga content. The higher the Ga content, the higher the pressure before the δ -phase transforms to a denser-state. The transformation path is dependent upon the overall Ga content of the δ -phase.

At a Ga content of 1.0 at. % Ga the transformation begins by forming a mixture of the α' -phase and the amorphous-state. For this alloy, the α' -phase and amorphous-state mixture is stable upon pressure release even after small incremental pressure cycles just above the initiation of the transformation. It is believed that the large amount of amorphous-state formed early in the transformation cycle for this alloy disrupts the crystallographic alignment between the martensitic α' -phase and the parent δ -phase and is responsible for the martensitic α' -phase not transforming back to the δ -phase upon pressure release.

At a Ga content of 1.7 at. % the δ -phase first transforms directly to the α' -phase. After about 50% α' -phase is formed, the transformation changes to a $\delta \rightarrow$ amorphous-state transformation with a little more α' -phase forming either from the δ -phase or the amorphous-state. The amorphous-state in this mixture begins to transform to the α' -phase at pressures of 5-7 kbars. Pressure release at low pressures, where little of the amorphous-state has formed, results in the martensitic α' -phase transforming back to the δ -phase. The amorphous-state in these two lower Ga alloys slowly crystallizes into the δ -phase upon heating. When the α' -phase transforms into the β -phase, near the normal $\alpha \rightarrow \beta$ transformation temperature, the rejected Ga moves into the amorphous-state causing it to spontaneously crystallize into the δ -phase. This behavior shows that the relative stability of the amorphous-state to that of the δ -phase is dependent upon the Ga content.

At 2.5 at. % Ga the δ -phase initially transforms to the α' -phase. Only as the pressure approaches 10 kbars and the amount of α' -phase approach 60 % does any significant amount of the amorphous-state form in this alloy, and only after a 10 kbar pressure cycle does the phase-mixture remain stable upon pressure release. Even after a 10 kbar pressure-cycle the martensitic α' -phase transforms directly back to the δ -phase when heated. It appears that at this alloy content enough amorphous-state forms at 10 kbars to disrupt the $\alpha' \rightarrow \delta$ transformation on pressure release, but not enough forms to disrupt the $\alpha' \rightarrow \delta$ transformation during the heating cycle. The small amount of amorphous-state that forms in this alloy crystallizes into the δ -phase over a wide temperature range extending even into the normal β -phase temperature range.

In addition to the transformation start pressure being dependent upon the Ga content, the rate at which the δ -phase transforms to a denser material is also dependent upon the Ga content. As one would expect, the δ -phase in the lower Ga content alloys transforms faster than in the higher Ga content alloys. As pointed out above the rate at which the δ -phase transforms does not necessarily relate to the rate of formation of the products of that transformation. The δ -phase is transforming to two products in the lowest Ga alloy, but is only transforming to the α' -phase early on in the transformations of the two higher Ga alloys.

The existence of the amorphous-state requires innovative new tools for identification and analysis. The density/compressibility data presented in this paper is one such tool for analyzing the amorphous-state, but it requires other knowledge of the material for proper analysis. Disordered states are common in irradiated materials. In the on-going studies of aging effects in Pu, the existence of radiation damage, and irradiation particles and effects requires careful examination for the possibilities of amorphous-state development.

Computation of Irradiation Damage in Alpha-Decay Actinides

I.I. Konovalov

All-Russia Scientific and Research Institute of Inorganic Materials (VNIINM), Rogov st. 5a
Moscow 123060 Russia

INTRODUCTION

Code VACS «Vacancy Activated Condense System» has been developed for calculation of microstructure parameters and properties change in metal nuclear fuel and structural materials producing inert gas atoms under neutron irradiation^{1,2}.

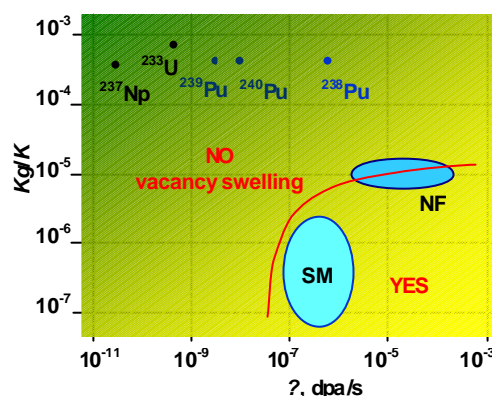
Use of code VACS for self-irradiated metal ^{239}Pu has shown certain conformity of calculated results and experimental data³. The code also has been used for calculation of structure change of alloys in hypothetical system $^{238}\text{Pu} - ^{239}\text{Pu}$ ⁴.

PHISICAL MODEL AND COMPUTAITION RESULTS

Basic thesis of calculation model used in code VACS are given. The kinetics of microstructure irradiation damage: concentration of point defects, density of loop and line dislocations, helium bubble morphology are calculated. The evaluation of influence of microstructure changes on macroproperties of some isotopes U, Np, Pu in metal form under long-life self-irradiation are discussed.

CONCLUSION

In studied field of isotopes physical parameters there are no areas of instable irradiation processes leading to accelerated vacancy swelling. Calculation results of structural changes in self-irradiating metals correspond to basic features of irradiation damage in metal nuclear fuels generating inert gas Xe, Kr and structural materials generating He in reactor core conditions.



The area of vacancy swelling in dependence of damage rate K and rate of inert atoms production Kg . SM – Structural Materials, NF – Nuclear Fuel.

1. I.I. Konovalov “Code VACS. Theory and Swelling Computation of Nuclear Fuel”, Moscow, VNIINM, 2001-3.
2. I.I. Konovalov, Proc. 23 RERTR Int. Meet., ANL/TD/TMDI-12, **135** (2001).
3. V.?. Orlov, I.I. Konovalov, S.A. Kisilev, et al. in Proc. V Int. Workshop “Fundamental Plutonium Properties”, Snezhinsk, Russia, Sept. 12-16 2005, **52** (2005).
4. I.I. Konovalov and V.?. Orlov in Proc. V Int. Workshop “Fundamental Plutonium Properties”, Snezhinsk, Russia, Sept. 12-16 2005, **54** (2005).

Friday, July 14, 2006

Lunch

Poster Session

Microscopy Events

Oral Presentation at Small Panel Discussion of LLNL Microscopy Capabilities

Transmission electron microscopy of actinide materials

Kevin Moore

Chemistry and Materials Science Directorate, L-350

Lawrence Livermore National Laboratory

In this presentation we will give a general overview of techniques available via transmission electron microscopy (TEM) for the interrogation of actinide materials: high resolution transmission electron microscopy (HRTEM), electron energy-loss spectroscopy (EELS), bright- and dark-field TEM, electron diffraction, and scanning transmission electron microscopy (STEM). We will show how each of these techniques can be utilized to investigate atomic and electronic structure, in turn illuminating the nano-scale and bulk properties of actinide materials.

Friday, July 14, 2006

Oral Session Two

Afternoon

Details of relativistic Hartree-Fock method as applied to crystals: Differences from density functional theory

A.L. Kutepov

Institute of Technical Physics (VNIITF), Snezhinsk, Russia

ABSTRACT

In this presentation the details of recently accomplished realization of relativistic Hartree-Fock method will be given. The purpose of creating of this new code is to study the effect of exact exchange on the calculated properties of actinides and also to be a starting point for developing of more sophisticated schemes with correlation included. The reason is that the widely used density functional theory (DFT) treats exchange in very simple form, which presumably may be source of the errors in applying it to actinides. Till now, HF method for crystals has been used mostly in the connection with LCAO (linear-combination-of atomic-orbitals), [1]. In LCAO basis, however, it is difficult to include relativistic terms due to analytical form of basis functions near nuclear (the variational collapse problem). Only recently, LMTO (linear-muffin-tin-orbitals) -based Hartree-Fock code has appeared, [2], and it was applied for 3d-metals. The code in [2] has, however, some restrictions, like ASA, and, also, it seems to be not fully relativistic, which is important for studying of actinides. So, it was decided to develop strict full-potential realization of Hartree-Fock (HF) method with the relativistic terms included. In the present code, the LMTO basis has also been used. Numerical form of LMTO basis functions inside muffin-tin spheres allows us to avoid the problem of variational collapse. In this new full-potential method the Metfessel's idea of interpolation was applied to calculate coulomb and exchange integrals and to represent density and potential in the interstitial region.

Though it is known, that exchange interaction in metals is well screened and, thus, correlation has to be included as well, the use of HF as first approximation has many virtues: well defined, yields variational total wave function (which is absent in density functional theory, for example), and is free of self-interacting (the well known problem in DFT). The effect of correlation may be studied then by, for example, some variant of Hedin's GW theory, [3].

1 R. Dovesi, C. Pisani, F. Ricca, C. Roetti, and V.R. Saunders, Phys Rev B **30**, 972 (1984).

2 I. Schnell, G. Czycholl, and R.C. Albers, Phys Rev B **68**, 245102 (2003).

Density-Functional Calculations of β -Pu-Ga (Al) Alloys

P. Söderlind^{*}, A. Landa^{*} L. Vitos[†]

^{*} Lawrence Livermore National Laboratory, Livermore CA 94552, USA

[†] Royal Institute of Technology, Stockholm, SE-10044, Sweden

At atmospheric pressure plutonium metal exhibits six crystal structures upon heating from room temperature to the melting point. The least dense phase (β -Pu, fcc) has a 25% larger volume than the ground-state (β -Pu, monoclinic) phase and is thermodynamically stable at temperatures between 593 and 736 K. In order to extend the stability of β -Pu to ambient temperatures, plutonium is alloyed with a small amount of so-called ' β -stabilizers', for example, Ga or Al. The β phase has no equilibrium solubility with any of these β -stabilizers but upon cooling of the β -Pu-Ga (Al) alloys, under certain conditions, Ga (Al) atoms can be trapped in the β lattice causing an expansion. An expanded monoclinic Pu-Ga (Al) phase is usually called "the β' phase". Hecker *et al.*¹ suggested that the enhanced volume of β' -Pu is solely due to the random distribution of Ga (Al) solutes in the monoclinic lattice and the unexpanded β lattice can be restored if the solute atoms are forced to move into preferred positions, e.g., during annealing. Recently, Sadigh and Wolfer confirmed this hypothesis by performing the plane-wave pseudopotential calculations for a variety of super-cell configurations². However, all these configurations reproduced specific ordering of the solute atoms (Ga) at the selected sites in the β -Pu monoclinic structure, and disordered Pu-Ga alloys could not be considered. This problem is solved in the present calculations.

We employed two complementary techniques: (i) the exact muffin-tin orbital method (EMTO)³ incorporated with the coherent potential approximation (CPA) to treat a compositional disorder and (ii) an all-electron full-potential linear muffin-tin orbital method (FPLMTO)⁴ that accounts for all relativistic effects in Pu. Both methods establish that a random distribution of Ga (Al) atoms in the monoclinic lattice of β -Pu results in a maximum expansion of this lattice. Any kind of ordering of Ga (Al) on the monoclinic lattice results in shrinking of the lattice constant in comparison with complete disorder of the solutes. The ordered β_8 -(Pu-Ga (Al)) configuration possesses the smallest lattice constant which is very close to that of pure β -Pu. In addition, energetics of the ordered and disordered configurations is discussed.

Acknowledgements: This work was performed under the auspices of the U.S. Department of Energy by the University of California Lawrence Livermore National Laboratory under Contract No. W-7405-Eng-48.

- 1 S.S. Hecker, D.R. Harbur, and T.G. Zocco, *Prog. Mater. Sci.* **49**, 429 (2004).
- 2 B. Sadigh and W. G. Wolfer, *Phys. Rev. B* **72**, 205122 (2005).
- 3 L. Vitos, in *Recent Research and Development in Physics* (Transworld Research Network Publisher, Trivandrum, 2004), Vol. 5, pp. 103-140.
- 4 J.M. Wills, O. Eriksson, M. Alouani, and D.L. Price, in *Electronic Structure and Physical Properties of Solids: The Uses of the LMTO Method*, edited by H. Dreysse, *Lecture Notes in Physics* Vol. 535 (Springer, Berlin, 2000), pp.148-167.

LANL Computational Theory

M. I. Baskes*, S. Y. Hu*, S. M. Valone*, and M. A. Stan*

*Los Alamos National Laboratory, Los Alamos, NM 87545 USA

The Pu-Ga system is perhaps the most complicated binary alloy system in nature. Not only does this system have important technological importance, but also scientifically it is extremely challenging. Previously we have used the Modified Embedded Atom Method (MEAM) to describe the behavior of both Pu and Ga. This method, though semi-empirical, is able to capture most of the important unusual behavior of both of these elements.

In this presentation we show the results of recent calculations using MEAM for various alloys (phases and composition) in this complex system. Results presented will include simple bulk thermal and mechanical properties such as specific heat, thermal expansion, and elastic constants for the solid phases. Two-phase equilibrium will be discussed with respect to melting and the predicted phase diagram. Predictions will be compared with experiment when available.

Peculiar magnetic ordering in $\text{Pu}_{0.95}\text{Ga}_{0.05}$ alloy at low temperature

V. Arkhipov^{*}, Yu. Zuev[†], F. Kassan-Ogly^{*}, A. Korolev^{*}, S. Verkhovskii^{*},
Yu. Piskunov^{*}, I. Svyatov[†]

^{*}Institute of Metal Physics, Ural Branch of RAS, Ekaterinburg, Russia

[†]Russian Federal Nuclear Center — Institute of Technical Physics, Snezhinsk, Russia

We report on dc magnetization, electrical resistivity and ^{71}Ga NMR results indicating on the formation of static magnetic order in δ -phase of $\text{Pu}_{0.95}\text{Ga}_{0.05}$ alloy at low temperature ($T < 10$ K) and magnetic field up to 1T.

FINE SPLITTING OF ENERGY LEVELS IN MANY-ELECTRON ATOMS AND IONS

O.B. Nadykto, B.A. Nadykto

RFNC-VNIIEF, Arzamas-16 (Sarov), Nizhni Novgorod region, 607190,
E-mail:nadykto@vniief.ru, Fax: 83130 45772

Ref. [1] suggests trial radial wave functions for one-electron ions in the form of the product of one-electron functions

$$R_{nl} = - \left(\frac{(n-l-1)!}{((n+l)!)^3 2n} \right)^{1/2} \left(\frac{2n}{x} \right)^{3/2} e^{-\frac{nr}{x}} \left(\frac{2nr}{x} \right)^l L_{n+l}^{2l+1}(2nr/x). \quad (1)$$

It is well known that in the relativistic approximation hydrogen-like ion energies are described by Dirac-Sommerfeld relation:

$$E(Z, n, k) = mc^2 \left[\left[1 + \left[\frac{\alpha Z}{n - k + (k^2 - \alpha^2 Z^2)^{1/2}} \right]^2 \right]^{-1/2} - 1 \right] \quad (2)$$

where n is the principal quantum number, $k = j + 1/2$, j is the quantum number of net moment (the sum of orbital moment and spin), α is the fine structure constant, m is electron mass, c is light velocity, Z is ion nuclear charge. For $k = n$ ($j = n - 1/2$)

In the semiempirical approach [2], when calculating energy of many-electron ions, not only Coulomb interaction, but also additional interaction between electrons from different shells, which depends on orbital quantum number l , is taken into account. In so doing the electron wave function parameter changes noticeably. The energy of states (both the ground state and excited states) of the outer electron of lithium-like ions is described in most cases with an accuracy better than 10^{-4} . When the energy description has been obtained, calculated fine splitting (7) agrees with the experimental value with an accuracy of $\sim 1\%$ or better without using any additional empirical parameters.

The distance between the extreme components of the triplet of states $1s^2 2pns \ ^3P_2 - \ ^3P_0$ is very close to the splitting of states $1s^2 2p \ ^3P_{3/2} - \ ^3P_{1/2}$ of lithium-like ions, that is this is the difference between energies of states $1s^2 2p(^3P_{3/2})ns - 1s^2 2p(^3P_{1/2})ns$. Attraction by the outer ns shell increases the wave function parameter of $2p$ electron as compared to state $1s^2 2p$, which leads to a decrease in its fine splitting. With increasing n the fine splitting of states $1s^2 2pns \ ^3P_2 - \ ^3P_0$ increases and approaches the value for states $1s^2 2p$. The distance between the extreme components of the triplet of states $1s^2 2p^2(^3P)ns \ ^4P$ is close to the difference between energies of states $1s^2 2p^2 \ ^3P_2 - \ ^3P_0$. Parameters of interaction of electrons in configurations $1s^2 2s 2pnl$ of boron-like ions had been selected, which were used in the calculations of multiply charged ion characteristics. The calculated intervals of fine splitting make a certain portion of interval $1s^2 2s 2p \ ^3P_2 - 1s^2 2s 2p \ ^3P_0$ of beryllium-like ions, which changes slightly due to interaction of $2s 2p$ electrons with outer nl electrons. The unusual behavior of the fine splitting with n can serve a distinctive feature of these states.

Energy required for knockout of electrons from inner shells of neutral atoms is significantly less (by up to 25%) than energy of ionization of ion, which outer electrons are removed in. This does not mean a smaller bond of knocked-out electron in neutral atom. In this case, when inner electron knockout takes place, bond energy of outer electrons in the final state increases due to increase in the charge acting on them by one. The final-state fine splitting depends mainly on energy of remaining inner electrons rather than on transition energy. The transition energy depends on aggregative or chemical state of material, i.e. on what the state of the outer electron shell is which the knocked-out inner electron has been brought into. The fine splitting of energy of inner states is essentially independent of these changes. The fine splitting is smaller significantly for the states of outer electrons than for inner electrons.

References

1. B.A. Nadykto // VANT. Ser. Teoreticheskaya i Prikladnaya Fizika. 1994. Issue 1. P. 32
2. B.A. Nadykto // UFN. 1993. V. 163, No. 9. P. 37-75.

Saturday, July 15, 2006

Oral Session Three

Morning

DYNAMIC MATERIAL PROPERTY EXPERIMENTS AT LLNL*

Kimberly S. Budil
University of California
Lawrence Livermore National Laboratory

In recent years, considerable attention has been focused on extending the study of fundamental materials properties into new regimes. While static techniques allow for high fidelity probing of materials under pressure, most dynamic experiments have relied on either surface diagnostics such as velocimetry or recovery and post-shot analysis. There are many insights that have been gained from such experiments but they do not allow the experimenter to probe into the interior of the material, at the appropriate length and time scales to observe the deformation of the material real time and *in situ*. The desire to understand the dynamic response of materials to dynamic deformation has necessitated the development of novel diagnostic techniques and new methods for putting samples under pressure. This talk will focus on recent activities by a number of researchers at LLNL to investigate novel techniques for dynamic deformation, to develop new diagnostic techniques, and to exploit new facilities for the study of materials under extreme conditions. Experimental science is closely integrated with theoretical model development and advanced simulation and some highlights from this will be presented. *This work was performed under the auspices of the U.S. Department of Energy by the University of California, Lawrence Livermore National Laboratory under contract No. W-7405-Eng-48.

Explosive experiments for studying dynamic properties of transition metals, some actinides, and alloys on their basis

E.A.Kozlov¹, V.I.Tarzhanov, V.G.Vildanov, V.M.El'kin,

Federal State Unitary Enterprise "Russian Federal Nuclear Center – Zababakhin All-Russia Research Institute of Technical Physics", Snezhinsk, Russia, 456770, P.O. Box 245
E-mail: kozlov@gdd.ch70.chel.su

Abstract

In this article, we give brief overview of some earlier published data demonstrating how mechanical behavior of some transition and 5f-metals, as well as alloys depend on the content of impurities and alloying elements, the blank fabrication technology, aging, pressure, temperature, low, and high strain-rate-deformations. Control over stability of mechanical properties, particularly the shear and spall strength of the material, is demonstrated to be of critical importance. Effect of phase transitions on the features of spherical shells behavior under explosive loading is shown to be possible.

Keywords: data storage materials (A), shock-wave loading (B), mechanical properties (C), strain, high pressure (D), spherical shock-wave recovery experiments (E).

1. Introduction. The transition 3d-, 4d-, and 5d-metals, as well as metals with f-electron shells, i.e. lanthanides and actinides, have complex phase diagrams and regular significant changes in physical, mechanical, and thermodynamic properties of each phase.

Plutonium shows the highest sensitivity to changes in pressure, temperature, content of alloying elements and impurity elements (metallurgical and/or radioactive nuclear decay products). Due to substantial, sometimes anomaly, changes in the properties of different phases of Pu and its practical significance, this actinide was studied most comprehensively. In particular, one investigated and analyzed:

- its phase diagram in the wide range of pressures and temperatures (P,T) using high static pressure methods and techniques;
- changes in mechanical (strength and plastic) properties at quasi-static and dynamic loading in the region of existence of each phase, both in the initial state before aging, and after long-term self-irradiation;
- isothermal, isentropic, and shock compressibility;
- sound velocities at atmospheric pressure and different temperatures, as well as in the shock-compressed states, etc.

The purpose of this work is to discuss the earlier published data on the behavior and properties of some transition and 5f-metals being of interest from the standpoint of fundamental research into actinides, as well as verification and validation of modern strength models, as well as 2D- and 3D- numerical codes.

¹ Corresponding author E-mail: kozlov@gdd.ch70.chel.su, Fax: +007(351-46)52070, Tel: +007(351-46)54572
Postal address: Russian Federal Nuclear Center-E.I.Zababakhin
Research Institute of Technical Physics,
Snezhinsk, Russia, 456770 P.O. Box 245

2. Mechanical properties of unalloyed Pu and some model materials

The papers [1-5] show that at static ($\dot{\epsilon} = 10^{-3}$ 1/s), as well as at high-rate ($\dot{\epsilon} \sim 10^2$ 1/s) loading, the unalloyed metal reaches the highest strength characteristics ($\sigma_{0,2}^c$, σ_B^c) in the region of α -phase existence.

The strength properties of the metal depend not only on the loading conditions (P, T, $\dot{\epsilon}$), but also on the initial value of density and the content of admixtures (C, Si, etc.; for example [1-3]). The sensitivity of strength properties to the content of admixtures and initial density is most conspicuous just for the α -phase. The rate of the strength characteristics decreasing at long-term aging (self-irradiation) correlates with the quality of the original unalloyed metal, i.e. the content of admixtures and residual high-temperature phases in the cast and static compressed metal before aging. The higher is the content of admixtures in the original unalloyed metal and the lower is its initial density, the higher is the rate of the strength characteristics decreasing at long self-irradiation. The tendency for systematic reduction of the shear and spall strength in unalloyed aged metal is detected also under its explosive loading [6]. Not only changes in strength and plastic properties of the unalloyed metal due to variations in the total content of admixtures (C and Si primarily), but also recovery of mechanical properties is shown to be possible due to vacuum refining through removal of decay products (He, Am, U) accumulated at long-term storage from the α -Pu lattice. Difficulties of work with chemically toxic and radioactive materials stipulate that inert materials would be preferably used for preliminary studying some phenomena in a special experimental set-up making phenomena most obviously observed.

In particular, the aluminum alloy AMg-6 is interesting as a model (surrogate) material for studying the degradation of strength properties ($\sigma_{0,2}$ and σ_B) at long-term (up to 10 years) and superlong (up to 100 and more years) storage under different temperatures. In this alloy being plastically deformed (cold-worked) in the original state, one experimentally registered the 30-40 % decrease of the conventional yield limit and the ultimate strengths, $\sigma_{0,2}$ and σ_B , in quasi-static tension tests before aging and after 10 years of aging [7]. The same work develops the method for predicting changes in mechanical properties during superlong (over 100 years) exposure or operation based on the experimental results obtained in [7,10] with the samples being stored for up to 10 years at room temperature and for up to 10^4 hours at $T=22, 70$ and 100 °C. Taking into account specifics of the recovery processes in the alloy AMg-6, one derived the generalized equation of recovery, which, in contrast to the Kuhlmann-Cottrell-Aytekin theory [8,9], accounts for the decreasing rate of recovery as the yield stress of the cold-worked alloy approximates the original value registered prior to deformation. The obtained phenomenological equations are qualitatively consistent with the available dislocation models of recovery, which hopefully could be used for a wider class of metals and alloys. If so, after model parameters are specified, these models can be used to predict the service life of items that operate under recovery conditions.

3. Model spherical explosive experiments

To estimate the potential effect of changes (during superlong aging or changes in the manufacturing technology of items) in the spall and shear strength of the shell material on its

behavior at spherical explosive compression, very interesting are comparative explosive experiments with recovery of shells (of high-purity unalloyed iron and some steels) after their fracture at high radii and convergence. These materials, i.e.

- coarse-grained and fine-grained unalloyed iron of high purity;
- 30KhGSA steel hardened up to HR_C 35...40 units;
- the same steel in the delivery state;
- austenitic stainless steel 12Kh18N10T

have close values of the initial density, but possess considerably different mechanical characteristics, namely, original deformation curves, spall and shear strength, presence of the known α - ε -phase transformation in the unalloyed Fe and steel 30KhGSA and its absence in the austenitic stainless steel 12Kh18N10T. Under identical conditions of explosive experiments, the shells made of these materials have the similar initial geometry and mass but behave differently under explosive loading (Fig.1).

When thin metallic shells are compressed (approximation of incompressible shells), their convergence dynamics is independent of the material properties but governed only by the relation between masses of the shell surface unit and the accelerating layer of the explosive (HE). In the experiments presented in Fig. 1, the explosive loading conditions are chosen so that

- the spall and shear fractures of different extent could take place in the material of all tested steel shells in the first-type experiments on high radii;
- and the regime of convergence up to the deep radius and recompaction of the shell material fractured at high radii could be ensured in the second-type experiments that differ from the first-type ones only by the presence of an outer case that restricts the released explosion products.

The comparative data given in Fig.1 for the unalloyed high-purity iron and hardened steel 30KhGSA clearly demonstrate that the spall and shear strength of the spherical-shell material cause significant specifics how their state changes both during the shock-wave acceleration, and the subsequent inertial convergence at two implosion regimes. The obtained systematic experimental results are of interest also from the viewpoint of verification and validation of the modern physical strength models and numerical 2D-, and 3D- codes.

The explosive experiments proposed in [11] and carried out in [12-14] have also made it possible to perform calorimetric measurements [13] of all investigated shells, as well as systematic materials-science investigations of recovered shells [14] with an aim to reveal how mechanical properties and phase transitions in the shell material effect not only incipient occurrence and development, but also recompaction of the spall and shear fractures originating at high radii.

Conclusions

The results of fundamental research how behavior and density of the shell depend on the spall and shear strength of its material during implosion are presented. These results emphasize actuality of systematic investigations into degradation of strength properties of materials at long-term storage. Obtained results are also interesting from the viewpoint of verification and validation of physical strength models and modern 2D-, and 3D- numerical codes.



a)



b)



c)



d)

Fig.1 Meridian sections of the spherical shells made of unalloyed high-purity iron (a, c) and high-strength steel 30KhGSA (b,d)

- a), b) – the first mode of explosive loading corresponding to formation in the shells of spall and shear fractures with guaranteed stop of the shells at high radii prior to focusing;
c), d) – the second mode of loading, which differs from the first one by the restriction of explosion products release; shown are the features of recompacting of materials of the shells fractured at high radii after their convergence up to deeper radii.

References

- [1] H.R.Gardner, Mechanical Properties. In: Plutonium Handbook, O.J.Wick (ed), 1980, p.59-100. The American Nuclear Society, La Grange Park, Illinois. USA
Plutonium Handbook, O. Wick (ed), v.2, Translated from English ed. By N.T. Chebotaryov, M. Atomizdat, 1972, 456 p.
- [2] H.R.Gardner, I.B.Mann, Mechanical Property and Formability Studies on Unalloyed Plutonium. In: PLUTONIUM – 1960, Comptes Rendus de la Seconde Conference Internationale sur la Métallurgie du Plutonium, Grenoble, France 19-22 avril, 1960, organisée par Societe Francaise de Métallurgie, commissariat a l'energie Atomique, E.Grison, W.B.H.Lord, R.D.Fowler (eds), Cleaver – Hume Press LTD, London, 1961, pp.513-570
- [3] S.E.Bronisz, The Mechanical Properties of Alfa Plutonium in Compression, J. Nucl. Mat., 1963, v.9, # 1, pp.101-106
- [4] S.S.Hecker, J.R.Morgan, Effect of Strain Rate on the Tensile Properties of α - and δ -Stabilized Plutonium, Plutonium and other Actinides. Proc. 5th Int. Conf. on Plutonium and Actinides 1975. Baden Baden, September 10-13, 1975. Amsterdam – New York, 1976, pp.697-709
- [5] S.S.Hecker, M.F. Stevens, Mechanical Behavior of Plutonium and Its Alloys. Los Alamos Science, 2000, # 26, pp.290-309
- [6] E.A.Kozlov, V.I.Tarzhanov, I.V.Telichko, D.M.Gorbachov, D.G.Pankratov. The Effect of Long Self-irradiation on Change in Shear Strength of Unalloyed Plutonium under its Explosive Loading. Proceedings of the V-th International Ural Seminar Radiation Physics of Metals and Alloys, Snezhinsk, 23 February – 1 March 2003, p.90-91
- [7] D.A.Mirzaev, Yu.D.Koryagin, Ya.S.Dobrynina, A.A. Zvonkov, Study and Modeling of Recovery in Alloy AMg-6 to Predict Operating Resource of Details of Aerospace Facilities. Physics of Metal and Metallography, 2004, v.98, No 2, p.11-18
- [8] D.Kuhlmann, G.Masing, J. Raffelsieper, Zur Theorie der Erholung, Zeitschrift für Metallkunde. 1949. Bd.40. S.241
- [9] A.H.Cottrell, V.Aytekin, The Flow of Zinc Under Constant Stress, J.Inst. Metals, 1950, v.77, p.389-422
- [10] Jr. E.R. Dix, Thermal Treatment of Aluminium Alloys, Trans. ASM (Seminar on Physical Metallurgy of Aluminium Alloys), 1949, 210 p.
- [11] E.A.Kozlov, Shock Adiabatic Features, Phase Transition Macrokinetics, and Spall Fracture of Iron in Different Phase States, High Pressure Research, 1992, v.10, pp.541-582
- [12] E.A.Kozlov, V.I.Tarzhanov, I.V.Telichko, D.M.Gorbachev, and D.G. Pankratov, Stress Relaxation of Elastic Precursor for Unalloyed Uranium and Some Uranium-based Alloys, Rep.Russ.Ac.Sci, 2006, v.408, No.3, pp.328-332 [Doklady Physics (Engl. transl.), 2006, Vol.51, No. 5, pp.252-256]
- [13] V.G.Vildanov, M.M.Gorshkov, E.A.Kozlov, O.V.Tkachov, D.T.Yusupov, Solid-State Calorimeter Technique for Measurements of Residual Energy of Shock Compressed Spheres and Shells. International Conference the VII-th Zababakhin Scientific Talks, September 8-12 2003, RFNC-VNIITF, Snezhinsk
- [14] E.A.Kozlov, S.A.Brichikov, D.M.Gorbachev, I.G.Brodova, T.I. Yablonskihk, Features of Incipient Occurrence, Development, and Recompaction of Spall and Shear Fractures in Shells of Unalloyed Iron and some Steels under their Spherical Explosive Loading, VIII Zababakhin Scientific Talks, September 5-10, 2005, RFNC-VNIITF, Snezhinsk, Russia, pp.172-173

Overview of some dynamic material properties research; continuum level to microscopic level

R. S. Hixson, DE-9, Los Alamos National Laboratory

Abstract

This presentation will focus on the use of shockwave and stress wave compression techniques, both conventional and creative, to produce a wide range of information to be used in the determination of materials Equations-of-state (EOS). This work supports the goal of creating multi-phase EOS's that are constrained by all available data. Typically static compression experimental techniques are used to map out material isotherms and locate phase transformations. But it is just as important to use dynamic data to locate relevant phase transformations, including melting, and to provide fundamental pure phase EOS information. The combination of static and dynamic data should provide crucial constraints on multi-phase EOS's

The use of conventional, macroscopic shock compression techniques for generating EOS data will be reviewed. In addition, the use of ramp wave compression data will be discussed, and compared to the shock data. Proposed new diagnostic techniques for detecting phase changes dynamically will be discussed, as well as some possibilities for making measurements at smaller length scales.

On the possibility of application of ultrashort pulses of laser radiation to study the properties of metallic Pu under extreme conditions

A.Ya. Uchaev, V.T. Punin, N.I. Sel'chenkova, E.V. Kosheleva

Russian Federal Nuclear Center – VNIIEF, Russia, 607188, Nizhni Novgorod region, Sarov, Mira avenue 37, uchaev@expd.vniief.ru

At present the knowledge of matter behavior under extreme conditions is acute as, for example, ultimate capabilities of current technology and unique scientific facilities are related to the processes caused by powerful impulse action on the matter.

The knowledge of behavior of metallic *Pu* under extreme conditions is acute at present due to insufficient knowledge of properties of metallic *Pu* of different age and its behavior at high-intense pulse action.

To study the dynamic failure phenomenon¹⁻³, there were applied the methods of explosion and shock-wave loading (longevity is $10^{-5} < t < 10^{-8}$ s), the heat shock method (HS - longevity range $t \sim 10^{-6} \div 10^{-10}$ s); as well as to study the dynamic failure in subnanosecond range ($10^{-9} \div 10^{-11}$ s), there were applied ultrashort pulses of laser radiation (USPLR) with power density J of laser radiation up to $J \sim 10^{14}$ W/cm².

The paper contemplates a possibility for applying the critical phenomena theory and theory of second-kind transitions to the description of failure process at the final stage in the dynamic longevity range (submicro-subnanosecond range).

As a result of a large scope of research^{1,2} it was shown that arising dissipative structure – failure centers cascade - puts up the resistance of the body to the external action in the dynamic longevity range. The failure centers cascade is a fractal cluster.

A model of lattice gas was applied for adequate mathematical modeling of the arising failure centers cascade which is a percolation cluster at the stage of macro-failure.

At present it is known that canonical distribution function in the Ising model is similar to the function of distribution of large canonical ensemble in the lattice gas model. This reflects the analogy between the model of Ising ferromagnet and the lattice gas model.

Application of the apparatus of critical phenomena theory and second-kind transition theory in an effort to describe the dynamic failure processes at the final stage allowed determination of universal attributes of metals behavior in the dynamic failure phenomenon conditioned by self-organization and instability in dissipative structures.

On the basis of complex approach to the work there is considered a possibility for obtaining quantitative characteristics of behavior of a number of metals including metallic Pu, under extreme conditions on the macro-level on the basis of analysis of quantitative characteristics of dissipative structures, arising on different scale levels, whose behavior is similar to behavior of systems near the second-kind transition.

The approach proposed specifies the possibility for predicting behavior of a number of metals, including metallic Pu⁴ on different scale-time levels basing upon experimental studies performed in the laboratory environment on small samples.

1. R. I. Il'kaev, A.Ya. Uchaev, S. A. Novikov, N.I. Zavada, L. A. Platonova, N. I. Sel'chenkova. Universal metal properties in the dynamic failure phenomenon // DAN, 2002, vol. 384 (3), P. 328-333.

2. R. I. Il'kaev, V. T. Punin, A. Ya. Uchaev, S. A. Novikov, E.V. Kosheleva, L. A. Platonova, N. I. Sel'chenkova, N. A. Yukina. Time regularities of metals dynamic failure process conditioned by hierarchic properties of dissipative structures – failure centers cascades //DAN, 2003, vol. 393 (3), P.326-331.
3. A.Ya. Uchaev, V.T. Punin, S. A. Novikov, E.V. Kosheleva, A.P. Morovov, L. A. Platononva, N. I. Sel'chenkova, N.A. Yukina. “Substantiation of the possibility of obtaining of quantitative characteristics of metals behavior under extreme conditions on the macro-level on the basis of regularities of behavior on meso-level”. Matter extremal states. Detonation. Shock waves. Proceedings of the International Scientific Conference, the VII Khariton Readings. 14-18 March 2005. Edited by the Doctor of Sciences, Engineering, A.L. Mikhailov. RFNC-VNIIEF Sarov. 2005. P. 356-361.
4. Plutonium Handbook A Guide to the Technology, volume I. Edited by O.J. Wick Pacific Northwest Laboratories Battelle Memorial Institute. 1967 by Gordon and Breach, Science Publishers, Inc. 150 Fifth Avenue, New York.

X-RAY DIFFRACTION STUDIES OF THE RELAXATION PROCESS OF DYNAMICALLY COMPRESSED CRYSTALS

L.A. Egorov, V.V. Mokhova

Russian Federal Nuclear Center All-Russia Research Institute of Experimental Physics
607190, Sarov, Nizhni Novgorod region, Russia

Abstract. Results from an X-ray diffraction structural study of crystals under shock-wave compression are presented. An analysis of the data leads to the conclusion that at the shock front, the crystals undergo universal structural changes over the entire range of pressures studied.

X-ray diffraction patterns suggest that the relaxation process of structural change is related to a change in the state of the crystal electron subsystem responsible for the chemical bonding in substance. The process of structural change at shock front can be divided into two stages: 1) uniaxial compression of the structure, the compression direction coincides with the direction of shock-wave propagation; 2) transformation of the unstable, uniaxially compressed, initial structure to a structure determined by the degree (depth) of relaxation of the electron subsystem responsible for the chemical binding of the ionic component of the crystal. X-ray diffraction patterns of a number of crystals at both stages of the process of structural change are presented.

Keywords: X-ray diffraction, dynamical compressed crystals, a relaxing process of substance.

Poster Session

VNIINM (Bochvar) Abstracts

A new method of describing uranium oxidation in water vapor

A. Karnozov (VNIINM)

Phase Transformations in Pu-Al and Pu- Ga Alloys. Effects of Pressure and Temperature on the Kinetics of the Delta-Phase Decomposition

L.F. Timofeeva

A.A.Bochvar VNIINM (All-Russian Research Institute of Inorganic Materials), Moscow, Russia

EVOLUTION OF PHASE DIAGRAMS UNDER PRESSURE

The binary phase diagram at atmospheric pressure as a section of the pressure–temperature - composition PTC diagram results from a regular variation of phase areas with space. PT diagram for Pu and earlier experimental data ^{1,2,3} underlie schematic phase diagrams for the Pu-Al and Pu- Ga systems over the 0 ~3 GPa pressure range (see Figure 1). As Pu phases disappear with increasing pressure, the binary phase diagram varies from complex one at atmospheric pressure to rather simple at high pressures (see Figure 1). Features of PT binary Pu-Ga (Al) diagrams was analyzed at the pressure of triple points on PT phase diagram for Pu. Our notions on the phase diagrams evolution under pressure were used for experimental constructing of phase diagrams at different pressures.

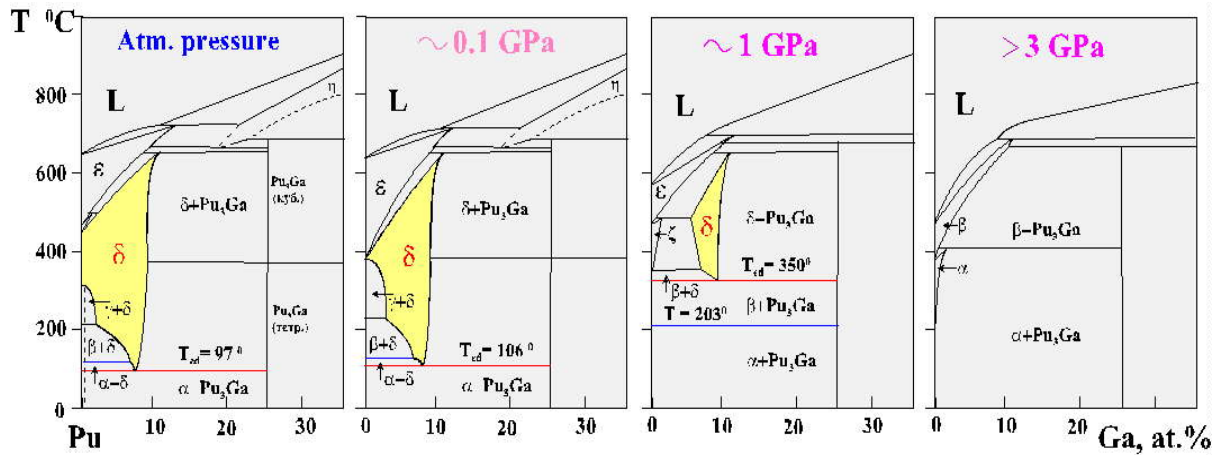


Fig1: Evolution of Pu-Ga Diagram under Pressure (scheme on a base of Experiment and Prognosis)

EXPERIMENTALLY AND THERMODYNAMICALLY DETERMINED δ-PHASE BOUNDARIES

Based on isothermal annealing results under static pressures as large as 0.6-0.8 GPa, δ-phase boundaries for the Pu-Al and Pu-Ga systems were delineated. The thermodynamic calculation of the displacement of the δ-phase boundaries to $P \cong 2-3$ GPa correlates well with the experiment. The δ-phase boundary shifts to higher concentrations of Al or Ga on the Pu-side and slightly to Pu on the intermetallic compound side. The δ-region decreases to the point of disappearance. The δ-phase eutectoid decomposition temperature at different pressures was evaluated from intersection of boundaries on the $N_{\text{MOЛЬ}}^{\text{Al(Ga)}} - 1/T$ K coordinates. The eutectoid decomposition temperature (T_{ed}) versus pressure was plotted (see Figure 2). Parameters of the four-phase equilibrium ($\delta, \alpha, \beta, \text{Pu}_3\text{Ga}$) at point “H” on PT binary PuGa diagram were determined. Point “H” is a projection on the PT plane of the HH line. It is line of intersection of two three-phase equilibrium surfaces on the PTC phase diagram (see Figure 3). Above and below point H the δ-eutectoid decomposition results in $\beta\text{Pu} + \text{Pu}_3\text{Ga}$ and $\alpha\text{Pu} + \text{Pu}_3\text{Ga}$, respectively.

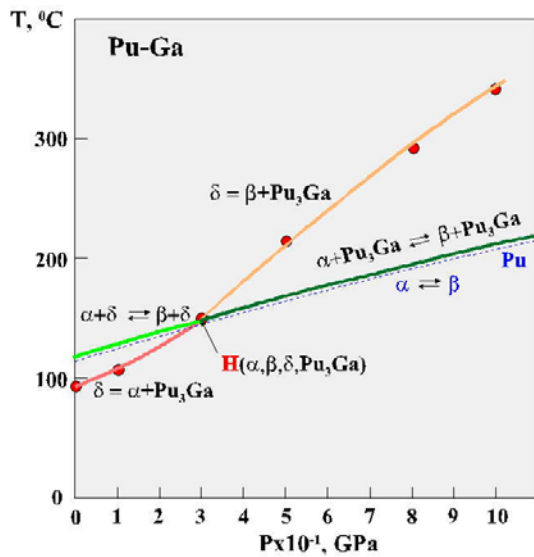


Fig 2: Effect of static pressure P on T_{ed} of PuGa alloys and $T_{\alpha \rightarrow \beta}$ Pu

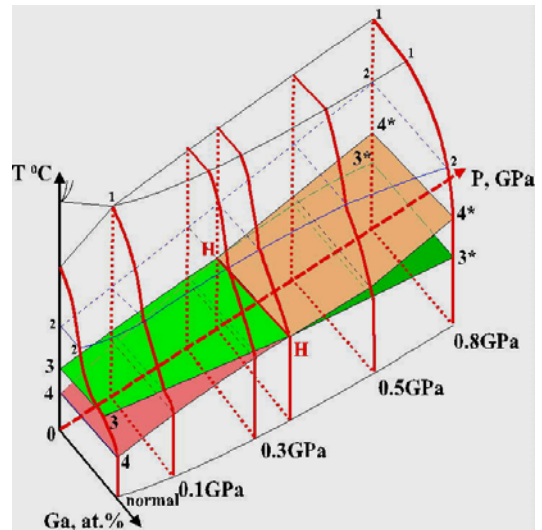


Fig 3: PTC diagram of PuGa- equilibrium
 $33HH-\alpha+\delta \leftrightarrow \beta+\delta$; $HH3*3*-\alpha+Pu_3Ga \leftrightarrow \beta+Pu_3Ga$;
 $44HH-\delta \leftrightarrow \alpha+Pu_3Ga$; $HH4*4*-\delta \leftrightarrow \beta+Pu_3Ga$

KINETICS OF δ -PHASE EUTECTOID DECOMPOSITION

As pressure and temperature increase, the rate of the δ -phase diffusion decomposition rises, the kinetics changes and the latent reaction period decreases from hundreds of hours to a few minutes as opposed to atmospheric pressure. The activation energy established for Pu-Al alloys by two methods, namely, the Avrami equation and the isothermal cross-section method, reduces from 30 kcal/mole at 0,1 GPa to 8 kcal/mole at 0,6 GPa. At a relatively low pressure, the both alloy systems show an eutectoid decomposition of different morphology: laminar for Pu-Ga (see Figure 4) and skeleton-like spheroidized for Pu-Al².

With due regard for decomposition acceleration and lower activation energy with increasing pressure, it can be suggested that the eutectoid decomposition can experience shock wave loading in a narrow pressure range.

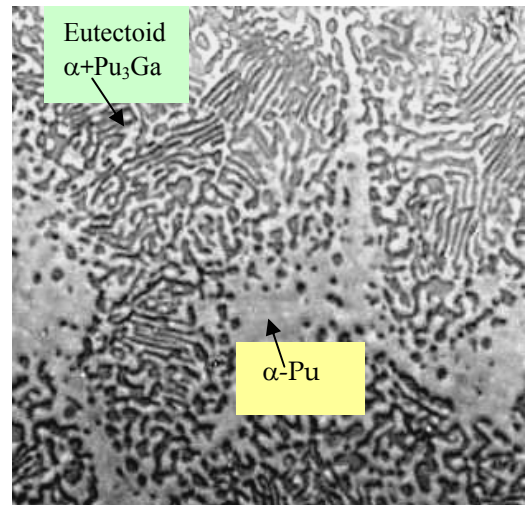


Fig 4: Microstructure of hypoeutectoid Pu-Ga alloy, $P \geq 1$ GPa

SUMMARY

Theoretical, experimental and thermodynamically calculated phase diagrams plotted for binary Pu-Al and Pu-Ga systems made it possible to clarify evolution of the phase regions under a pressure up to 2-3 GPa, to establish the temperature and pressure dependence of the eutectoid decomposition temperature. With increasing pressure, the δ -phase diffusion decomposition was shown to accelerate and the eutectoid decomposition to transform at relatively low pressures, resulting in an decrease in the activation energy.

- 1 N.T.Chebotarev, V.S.Kurilo, L.F.Timofeeva, M.A. Andrianov, V.V.Sipin .VANT(rus), seria: Materialovedenie. **37**, (1990).
- 2 L.F. Timofeeva, *in*: Ageing Studies and Lifetime Extension of Materials, ed. L. Mallinson, N-Y: Kluwer Academic /Plenum, (2001).
- 3 L.F. Timofeeva. Metallovedenie i termicheskaya obrabotka (rus). **11**, (2004).

The Application of Thermodynamic Approach for Development of chemically stable soft X-Ray Multilayer Mirrors Based on depleted Uranium

A.L.Udovsky^{*)}, I.A.Artioukov^{**)}, R.M.Fetchenko^{**)}, Y.A.Uspenski^{**)}, A.V.Vinogradov^{**)}

^{*)} Baikov Institute of Metallurgy and Materials Science of RAS, Leninsky Prosect, 49, Moscow 119991, Russia

^{**)} P.N.Lebedev Physiacl Institute of RAS, Leninsky Prospect, 53, Moscow 119991, Russia

Progress in ultrathin film deposition, which has been going on over three decades, resulted in development of normal-incidence X-ray optics based on multilayer coatings. The examples of the X-ray optics applications are:

a) space telescopes providing X-ray images of the Sun and stellar objects with angular resolution down to 0.5 arcsec, b) analytical fluorescence and microprobe equipment, instrumentation for synchrotron radiation and plasma physics, c) extreme ultraviolet (EUV) projection lithography, d) condensed matter physics, e) extreme ultraviolet optics, and f) cell biology.

Another frontier where normal incidence optics is expected to work is interval 3-6 nm. The wavelengths near carbon K-edge (energy $E \approx 280$ eV, wavelength $\lambda \approx 4,4$ nm) are particularly promising for material and biological applications due to their deep penetration into polymer, organic and biological samples.

Use of depleted uranium and uranium-base chemical compounds is shown to significantly increase the performance of multilayer mirrors intended for the wavelengths 3-6 nm. In comparison with multilayer mirrors based on 3d-elements increase of peak reflectivity is of factor 1,3, while the integral reflectivity increase by factor 2. The high chemical reactivity of pure depleted uranium hampers its usage. However many chemical depleted uranium compounds are chemically compatible with carbon that makes possible the fabrication of high – quality depleted uranium – based multilayer coatings.

For instance, XANES, XRF and EXAFS measurements near and below the carbon K-edge have become important techniques for investigations of many kinds of organic and inorganic materials. The maximum of normal incidence reflectivity achieved so far is about 13%. This result, which was obtained with Fe – C and Cr – C coatings, is three times lower than theoretical predictions for these multilayers. Insufficient reflectivity severely hinders the construction of high throughput and high spatial resolution imaging systems and, consequently, limits the field of possible applications at these wavelengths.

New material-pairs featuring better optical or technological properties may be of great use for the improvement of multilayer X-ray mirrors. From this point of view it is important to extent the scope of possible material-pars combination by including chemical compounds and “exotic” materials. One of such materials is depleted uranium that has been utilized in various civilian fields benefiting from its high density and low radioactivity. In paper [1] we have considers depleted uranium compounds as possible components of material-pars for multilayer mirrors intended for the wavelengths 3-6 nm and especially for $\lambda \approx 4,5$ nm. In paper [1] we have analyzes the optical properties of depleted uranium and highlights its potential for SXR optics. The great advantage of the uranium and its compounds, which determines its higher potential, arises from much lower absorption in U and its compounds than in 3d-metals. This advantage of U holds at all the wavelengths between 3.0 nm and 6.0 nm. One more argument in favor of uranium originates from its large atomic volume. The large volume makes the density of uranium atoms insensitive to formation of a compound making possible to vary the composition of uranium compounds to achieve both good X-ray characteristics of uranium containing layers and their compatibility with a spacer material. By comparison, the atomic volume of 3d-metals is 1,7-1,9 times lower uranium and its chemical compounds can be used with both carbon and Si. But to do grounded predicted of multilayer performance, the laborious analysis of optical, chemical and thermodynamic and other properties of materials is required.

A fast decrease of reflectivity in short period multi-layers with the growth of roughness and layer mixing imposes stringent demands on material selection. The chemical compatibility of partner materials connected with diffusion processes, chemical interactions and re-crystallization going at interfaces and in layers. At the present day the specific features of these processes arising from spatial scale of 1 nm are insufficiently studied. In view of this, it is reasonable to base the chemical compatibility analysis on the thermodynamics of multi-component systems, despite the fact that most thermodynamic data were obtained from experiments carried out on the scale 1 μ m or more. This thermodynamic approach is applied to consider the compatibility of depleted Uranium – base materials with carbon in multiplayer mirrors for the wavelength 4,5 nm.

The high reactivity of pure uranium gives no ways to use this material as pure component of short-period multiplayer mirrors. The nature of this reactivity is given by a formation enthalpy at room temperature of some uranium compounds: - 67,8 for UO (meta-stable compound), - 69,6 for UN and -23,0 for UC in Kcal/mole. The formation enthalpy of UO₂ is even higher, - 86,5 Kcal/mol. UO₂. The oxidation to UO₂ determines the self-ignition of pure uranium under moderate heating in air. The temperature of this reaction sensitively depends on the sample surface. For example, a cube of uranium with the surface 0,2 cm²/g ignition at 600°C, while an uranium film with the surface 50 cm²/g does at 350°C [2]. This high reactivity of pure uranium necessitates turning to depleted uranium compounds as best components of multiplayer coatings intended for λ = 4,5 nm. As is shown in paper [1] that UN-C multi-layers can show high peak and integral reflectivity. However the use of uranium mono-nitride may cause technological problems [3-4], because the free energy of formation for the compounds UN, UN_{1,55}, UN_{1,6} and UN_{1,65} compositions are nearly equal and partial pressure of nitrogen over UN surface is high [2]. These factors strongly hamper the fabrication of the stoichiometric UN target and the deposition of homogeneous UN layers. The use of UC, which also promises high reflectivity [1], is more justified from technological point of view. It is known [5] that UC in mixture with U₂C₃ hardly oxidizes in air and may be perfectly protected by a thin carbon layer.

A more comprehensive analysis of the compatibility of depleted uranium carbides layers may be done with the phase equilibrium diagram of the U-C system. The phase diagram of the U-C system accordingly by Storms [5] shows that UC and C are not in chemical equilibrium. However in work [6] by using thermodynamic analysis was shown that U₂C₃ dissociates on UC and graphite at the temperature 1180°C. Later in reference book [7] also have been published and also shown that the U₂C₃ dissociates on the same phases at the temperature 850°C. But in paper [8] by CALPHAD-methodology has been calculated of the phase diagram of the U-C system, which has not confirmed the results got in works [6,7] In this connection is required realize the additional studies concerning clarifications of the question for stabilities of the U₂C₃ within the range of low temperature (from room temperature up to 850 or 1100°C).

This work was supported by Russian Basic Research Foundation Projects N 02-02-16599-a, 03—02-16438-a, 01-02-17432-a, Russian Federal Target Program “Integration” (Grant B0056)

References

1. I.A.Artioukov, R.M. Fetchenko, A.L.Udovskii, Yu.A.Uspenskii, A.V.Vinogradov. “Soft X-ray multilayer mirrors based on depleted uranium”. Nuclear Instr. And Methods in Physics Research v.217, 2004, p.372-377.
2. Yu.N. Sokurski, Ya.M. Sterlin, V.A. Fedorchenko, Uranium and its alloys, Moscow, Atomizdat, 1971 (in Russian).
3. M.K.Urry. “Optical Constants of Uranium Nitride Thin Films in the EUV (80-182eV)”.
4. L.Black, et al. J. of Alloys and Compounds, v.315 (2001) p.36-41.
5. E. Storms, The refractory carbides, Academic Press, NY, 1967.
6. A.L.Udovsky. The thesis for a Doctor's degree. 1985.
7. Binary Alloy Phase Diagrams. Second Edition, Ed. T.B.Massalsky, Ohio (1990) 892-893.
8. P.Y.Chevalier, E.Fisher. Thermodynamic modeling of the U-C and U-B binary systems.

Poster Session

VNIIEF (Sarov) Abstracts

INSTABILITY OF ACTINIDE ELECTRON STRUCTURE UNDER HIGH PRESSURE

B.A. Nadykto

RFNC-VNIIEF, Arzamas-16 (Sarov), Nizhni Novgorod region, 607190,
E-mail:nadykto@vniief.ru, Fax: 83130 45772

1. Refs. [1], [2] show the course of transformation of four plutonium-gallium alloys with 1, 1.7, 2.5 and 3.5 at. % Ga under isostatic pressure at 25°C in Bridgman dilatometer. As expected, large-volume δ phase collapses at low enough pressures and transfers directly from δ to α' phase with possible γ' -phase traces. Everything indicates that $\delta \rightarrow \alpha'$ transformation proceeds by the martensite mechanism much like it has been found in cooling.

The data presented shows that when δ -phase alloy volume changes under applied positive pressure above a body the work is done which is expended for the $\delta \rightarrow \alpha'$ transformation. This means that the energy level of the alloyed δ -phase is lower than that of the α' phase.

The presented curves can be used to determine the energy of the $\delta \rightarrow \alpha'$ transformation as a function of gallium concentration in alloy through calculation of $\int PdV$ at the inelastic segment of the compression curve. Energy per gallium mole in alloy is almost independent of gallium content, which suggests the existence of some stable gallium complex in δ plutonium, which manifests itself identically in alloys with Ga content ranging from 1 at. % to 3.5 at. %. Energy of this complex can be represented as: $\Delta E = 67 - 100x$ kJ/mole Ga, where x is the relative fraction of Ga in Pu-Ga alloy. In this case the enthalpy of intermetallic compound Pu_3Ga is 42 kJ/mole, which is close to the data evaluated in the literature [4].

If it is taken that in gallium-stabilized δ phase there is chemical bond of gallium and plutonium similar to that in Pu_3Ga , while in the α' phase the chemical bond disappears, then Helmholtz free energy difference evaluated experimentally from the $\delta \rightarrow \alpha'$ transformation under pressure at constant temperature is close to plutonium-gallium alloy formation enthalpy. Two experimental points obtained with the method of drop calorimetry [5] fall exactly on this calculated curve. In other words, the results of the measurements and experiments on the $\delta \rightarrow \alpha'$ transformation under pressure agree.

2. The recent experiments using diamond anvils and synchrotron radiation sources have supplied interesting, important information about crystalline and electron structure of actinides in the megabar pressure range [6-10].

Ref. [7] studies compressibility of Pa to 129 GPa pressure. The computational analysis shows that up to $P \approx 95$ GPa the experimental points fall on the computed curve with parameters $\rho_0 = 15.37$ g/cm³ and $B_0 = 115$ GPa. At higher pressures the experiment deviates significantly from the computed dependence and can be described as the state of another Pa electron phase with parameters $\rho_0 = 19,827$ g/cm³ and $B_0 = 400$ GPa. Ref. [7] notes that at $P = 77$ GPa the tetragonal structure of protactinium changes to low-symmetry orthorhombic structure of α uranium. At 77 GPa, however, there is no noticeable change in slope of the curve $P(\rho)$, which is evidence that the initial electron structure of Pa remains unchanged. The slope and electron structure change abruptly at 95 GPa, evidently, at unchanged orthorhombic crystalline structure. Previously [11] it was noted that the experimental data on compressibility of thorium and uranium also indicated the existence of a stiff phase in them (with $B_0 = 400$ GPa) at pressure above 100 GPa.

Compressibility of curium metal to 100 GPa pressure is studied in ref. [10]. The parent phase of Cm (of equilibrium density 13.3 g/cm^3) has bulk modulus $B_0 = 40 \text{ GPa}$, which is somewhat higher than that of americium metal and δ -phase plutonium. At pressure about 10 GPa the electron structure of Cm metal changes. The new phase parameters are $\rho_0 = 13.96 \text{ g/cm}^3$, $B_0 = 60 \text{ GPa}$. According to [10], at 17 GPa the parent binary hcp structure changes to fcc structure. In the 10-37 GPa pressure range, however, the experimental points are described well as states of one electron phase. No monotonicity of $P(\rho)$ is observed in the crystalline rearrangement at 17 GPa. Phase CmIII (monoclinic structure) has somewhat lower bulk modulus ($B_0 = 53 \text{ GPa}$) at the same equilibrium density ($\rho_0 = 13.96 \text{ g/cm}^3$). For $P > 57 \text{ GPa}$ the points for phases CmIV CmV can be described as states of one and the same electron phase with $\rho_0 = 20.35 \text{ g/cm}^3$, $B_0 = 280 \text{ GPa}$. The parameters of this electron phase are close to those of phase Am IV at pressure 55-100 GPa.

At standard conditions, there are three electrons in the outer shell in thorium metal and four in uranium. In compression by high pressure the electron structure rearrangement takes place leading to the increase in the number of outer electrons to five or even six. In americium and curium the number of outer electrons increases under pressure to five.

References

1. S.S. Hecker, D.R. Harbur, T.G. Zocco. Phase stability and phase transformation in Pu-Ga alloys. // *Progress in Materials Science*. 49 (2004) 429-485.
2. S.S. Hecker, D.R. Harbur, T.G. Zocco. Phase stability in plutonium-gallium alloys. // *Proceedings of International Workshop "Fundamental Properties of Plutonium"*, Sarov, 30 August – 2 September 2004. P. 3.
3. S.S. Hecker. Plutonium and its alloys. // *Los Alamos Science*. 26. 2000. P. 290.
4. ХИМИЯ АКТИНОИДОВ. Т. 2. Ред. Дж. Кац, Г. Сиборг, Л. Морсс. М.: Мир. 1997. С. 558-621.
5. Stan M., Baskes M.I., Muralidharan K., Lee T.A., Hu S., Valone S.M. Thermodynamic properties of Pu-Ga alloys. // *Fundamental Plutonium Properties. Abstracts of V International Workshop, September 12-16, 2005. Snezhinsk. Russia*. P. 73-75.
6. Vohra Y.K., Akella J. *Phys. Rev. Lett.* 1991. V. 67. P. 3563
7. Haire R.G., Heathman S., Idiri M., Le Bihan T., Lindbaum A., Rebizant J. *Phys. Rev.*, 2003, B67, 134101
8. Le Bihan T., Heathman S., Idiri M., Lander G.H. et al. *Phys. Rev.*, 2003, B67, 134102
9. Lindbaum A., Heathman S., Litfin K. et al. // *Phys. Rev.* 2001. Vol. B63. 214101
10. Heathman S., Haire R.G., Le Bihan T., Lindbaum A. et al. // *Science*. 2005. Vol. 309. P. 110-113.
11. Nadykto B.A., Nadykto O.B. // *Plutonium Future – Science 2003. Conference Transactions*. Ed. by G.D. Jarvinen. Albuquerque. New Mexico, USA, July 6-10, 2003. P. 184-186.
12. Akhachinskiy V.V., Timofeeva L.F. // *Thermodynamic of Nuclear Materials*. 1979. Proc. of Sympos. Julix, 29 Jan. – 2 Feb. 1979. Vol. II. IAEA, Vienna, 1980. P. 161-169.

SHS method for immobilization of plutonium-containing waste

Levakov Eu.V., Postnikov A.Yu.

(RFNC - VNIIEF, Russia, Sarov)

Glagovskyi E.M., Kuprin A.V., Bogdanov A.I., Pelevin L.P.

(VNIINM, Russia, Moscow)

The main results of work in the area of technology development for immobilization of highly active waste (HAW) and, in particular plutonium-containing ones into mineral-like array compounds using the method of self-spreading high-temperature synthesis (SHS) are presented.

The choice of mineral-like arrays for HAW immobilization is proved. According to the results of thermodynamic calculations the availability of systems' formation based on zirconolite, pyrochlorine and other mineral-like compounds under SHS mode has been shown. The conditions influencing on both characteristics of SHS systems combustion and quality of obtained materials have been studied to optimize the technological parameters of SHS mineral-like arrays.

Base technological modes for SHS compacting of arrays based on pyrochlorine containing HAW simulators have been tested.

It is shown that the parameters of hydrothermal stability of arrays formed by SHS methods are similar to the same ones in arrays got by the method of cold compacting- sintering. Based on the experimentally got results the stands for immobilization of HAW simulators by SHS have been created.

Experiments and model of dynamic deformation of U-238 and its alloy with Mo

B.Glushak, V.Pushkov, O.Ignatova

Russian Scientific-Research Institute of Experimental Physics, 607190, Sarov, Russia

INTRODUCTION

The results presented in this communication were gained by an analysis of the dynamic diagrams of uniaxial compression and tension of U-238 and its alloy with Mo (~1 wt %). The yield strengths presented in this study were assessed from the diagrams at different strain rates of $\dot{\epsilon} \leq 1800$ 1/s and initial temperatures $T \leq 600^\circ\text{C}$. The data obtained served as a basis for a semi-empirical model at the heart of which was an equation of state of U-238 and its alloy with Mo^{1,2}. Measurements were taken by the split Hopkinson pressure bar (SHPB) method³.

EXPERIMENTAL RESULTS

Compression. Yield strengths $\sigma_{-0.2}$ calculated from the σ - ϵ diagrams at different $\dot{\epsilon}$ and T values for uranium and its alloy with Mo are summarized in Table 1. The yield strength $\sigma_{-0.2}$ of the uranium alloy with molybdenum increased in proportion to the strain rate $\dot{\epsilon}$ and decreased almost linearly with increasing temperature^{2,3}.

Tension. The yield strength and tensile strength of uranium measured at $T \sim 0^\circ\text{C}$ and $\dot{\epsilon} = 1000$ 1/s were $\sigma_{+0.2} = (470 \pm 78)$ MPa and $\sigma_{+B} = (650 \pm 83)$ MPa, respectively. The samples failed at a percent elongation from 4,0 to 4,2%. The yield strength and tensile strength of the uranium alloy with Mo were $\sigma_{+0.2} = (900 \pm 56)$ MPa and $\sigma_{+} = (1080 \pm 62)$ MPa, respectively, at $T \sim 0^\circ\text{C}$ and $\dot{\epsilon} = 1200$ 1/s. The samples were destroyed at a percent elongation of 15%^{1,2,3}.

Table 1. Yield strengths data

T, °C	U-238		U-238+Mo	
	$\dot{\epsilon}$, 1/s	$\sigma_{-0.2}$, MPa	$\dot{\epsilon}$, 1/s	$\sigma_{-0.2}$, MPa
20	100-420	565±42	280-360	760
	1300-1600	660±80	600-880	868±54
			1000-1400	990±70
100	520-1040	446±48		
200	160-1440	440±30	350-510	580±30
			800-1100	665±18
			1300-1800	720±67
400	540-890	300±13	200-520	370±40
			800-1000	426±52
			1200-1700	500±35
600			200-500	275±35
			850-1000	330
			1200-1400	360±26

MODEL FOR DYNAMIC DEFORMATION OF U-238 AND ITS ALLOY WITH MO

Consider U-238 and its alloy with Mo as an elastoplastic medium such that its stress strength σ_i can be represented as a function of four variables defining its strained state; in the simplest case, σ_i is a product of four simple functions f_i , each dependent on only one variable^{2,4}:

$$\sigma_i = \sigma_i(\epsilon_i, \dot{\epsilon}_i, P, T) = A f_1(\epsilon_i) f_2(\dot{\epsilon}_i) f_3(P) f_4(T) \quad (1)$$

Function $f_1(\epsilon_i)$ in Eq.(1) allows for strain strengthening, $f_2(\dot{\epsilon}_i)$ and $f_3(P)$, for the effects of the rate of plastic strain and pressure, respectively, and $f_4(T)$, for thermal softening. Function $f_3(P)$ looks as^{2,5} $f_3(P) = 1 + \sigma_0 P$, where $\sigma_0 = \text{const}$.

Dependence (1) was approximated by the following analytical function

$$\sigma_i = A \cdot [1 + a(\dot{\epsilon}_i)^m] \cdot \left[\frac{T}{T_{ml}} \right]^n + b \left[\frac{T}{T_{ml}} \right]^k \cdot \left[\frac{\dot{\epsilon}_i}{\dot{\epsilon}_{i0}} \right]^l + c \ln \frac{\dot{\epsilon}_i}{\dot{\epsilon}_{i0}} \cdot f_3(P); \quad (2)$$

here, A, a, b, c, d, n, m, l, and k are constants, $\dot{\epsilon}_{i0} = 1 \text{ s}^{-1}$, and T_{ml} is the melting point.

Poisson's ratio ν is supposed to be a linear function of temperature, $\nu = 0,205 + 8,7 \cdot 10^{-5} T$, where ν is an absolute temperature. By way of illustration, the experimental values of the conditional yield strength $\sigma_{-0,2}$ measured under dynamic compression are compared to their theoretical counterparts² calculated from Eq.(2) in Figure 1.

The range of validity of the proposed model for dynamic deformation of U-238 and its alloy with Mo is²: $\sigma \leq 5 \text{ G}$, $\epsilon_i \leq 0,12$, $\dot{\epsilon}_i \leq 2 \cdot 10^3 \text{ 1/s}$, $293 \leq T \leq 873 \text{ K}$.

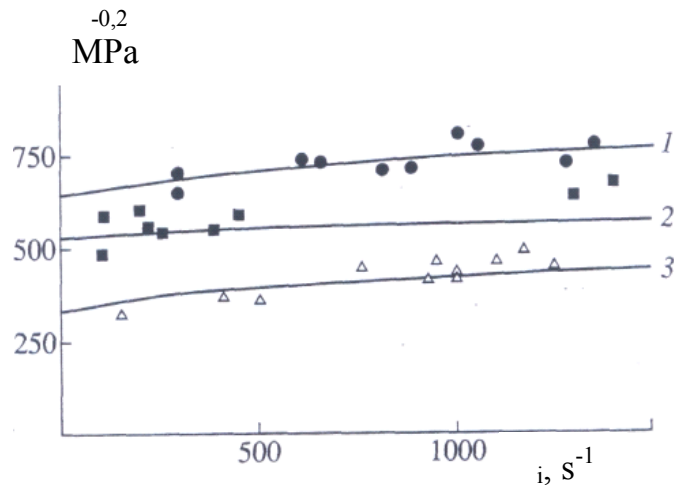


Fig 1: Conditional yield strength in the case of dynamic compression: (1)- $T=293\text{K}$, U-238+Mo; (2)- $T=293 \text{ K}$, U-238; (3)- $T=673\text{K}$, U-238+Mo; (○, □, △) experimental data; solid curves were calculated.

1. B.L. Glushak, *et al.*, Proceedings of abstracts of papers for the XIV International Conference "Effect of intensive flows of energy on substance", Terskol, Russia, 96, (1999).
2. S.A. Novikov, V.A. Pushkov, *et al.*, J. Chemical Physics (Rus), **18**, 10, 22-25, (1999).
3. S.A. Novikov, V.A. Pushkov, *et al.*, Mechanical Properties of Uranium under Quasi-static and Shock-Wave Loading, Preprint No.54-97, Russia, RF Nuclear Center: Scientific-Research Institute of Experimental Physics, (1997).
4. D. Steinberg, S. Cochran, and M. Guinan, J. Appl. Phys., **51**, No.3, 1498, (1980).
5. B.L. Glushak, O.N. Ignatova, J. VANT (Rus). Matematicheskoe Modelirovanie Fizicheskikh Protssessov, **2**, (1998).

Poster Session

VNIITF (Snezhinsk) Abstracts

On the feasibility of inelastic neutron scattering experiments on ^{239}Pu -based materials

E. Clementyev*, A. Mirmelstein*, and I.L.Sashin†

*Russian Federal Nuclear Center - Institute of Technical Physics, 456770 Snezhinsk, Russia

†Joint Institute for Nuclear Research, 141980 Dubna, Russia

Excitation spectra are indispensable experimental data to the understanding of the ground state and the major interactions in plutonium and plutonium-based compounds. In particular inelastic neutron scattering (INS) experiments can yield valuable answers with respect to the puzzling question raised over the absence of any evidence of magnetic moments in plutonium [1]. Detailed INS studies of the lattice dynamics are of high demand with respect to the origin of the structural phase transitions in Pu and the role of the electron-phonon coupling. Despite of the impressive range of information which has been attained by measurements of physical properties and theoretical studies, the investigation of the dynamic properties of plutonium is by no means complete [2]. INS is very limited in the case of plutonium to say it soft and almost nothing is known on the magnetic spectral response in this metal. As far as the lattice dynamics is concerned, experimental

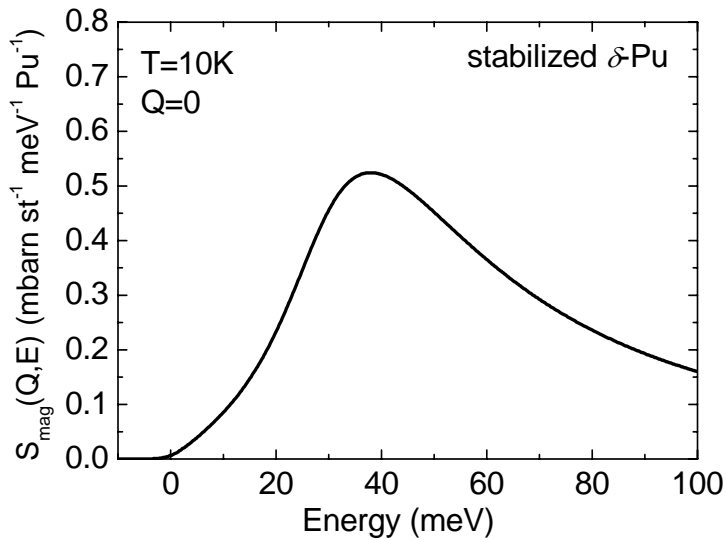


Fig 1: Calculated magnetic spectral response in fcc Pu at T=10K [6].

information on the phonon density of states and phonon dispersion in Pu is rather scarce [3,4]. Taking away the nonproliferation issues the main obstacle for INS in Pu-based materials is a huge value of the neutron absorption cross-section of the most common and most cheap ^{239}Pu isotope. For thermal neutrons $\sigma_{\text{abs}}(^{239}\text{Pu}) = 1017$ barns, two-three orders of magnitude higher than in the majority of the periodic table elements. Another important aspect is the energy transfer range to be studied. The magnetic spectral response in fcc Pu has been calculated (Fig. 1) on the basis of the experimental data for other strongly correlated electron systems, in particular CeNi [5] with the characteristic Kondo energy scale and the Sommerfeld coefficient very similar to $\delta\text{-Pu}$. The most promising energy transfer range in this system seems to be $0 < E < 100$ meV [6]. In $\alpha\text{-Pu}$ the corresponding neutron energy transfer range extends up to several hundred meV. The phonon energy cut-off in Pu is about 12 meV [3,4]. In Pu-based intermetallics the phonon spectrum covers a few tens meV. To sum up, in $\delta\text{-Pu}$ the energy transfer up to 100 meV is required to study both the magnetic and lattice dynamics.

Elastic neutrons scattering experiments on ^{239}Pu -based samples have been undertaken several times with a rather successful outcome (for example, see [7]). It is well known that the counting rates in typical elastic neutron scattering measurements are several orders of magnitude higher than in the case of the INS studies. To the best of our knowledge, nothing is published on the INS experiments on ^{239}Pu isotope. Another isotope, namely low absorbing ^{242}Pu , was used (see [4,8]). The difficulties of the INS studies of ^{239}Pu systems are remarkable, however we think that such an experiment is feasible. In fact ^{239}Pu is not unique in terms of a huge neutron absorption cross-section, natural Gd, Sm, Eu and B are all very bad elements for the INS technique. A formula unit of MgB_2 has a value of $\sigma_{\text{abs}}(\text{MgB}_2) = 1534$ barns, even higher than 1017 barns for ^{239}Pu . At the same time the total nuclear cross-sections are: $\sigma_{\text{s}}(\text{MgB}_2) = 14.19$ barns, $\sigma_{\text{s}}(^{239}\text{Pu}) = 14.19$ barns. We

information on the phonon density of states and phonon dispersion in Pu is rather scarce [3,4]. Taking away the nonproliferation issues the main obstacle for INS in Pu-based materials is a huge value of the neutron absorption cross-section of the most common and most cheap ^{239}Pu isotope. For thermal neutrons $\sigma_{\text{abs}}(^{239}\text{Pu}) = 1017$ barns, two-three orders of magnitude higher than in the majority of the periodic table elements. Another important aspect is the energy transfer range to be studied. The magnetic spectral response in fcc Pu has been calculated (Fig. 1) on the basis of the experimental data for other strongly correlated electron systems, in particular CeNi [5] with the characteristic Kondo energy scale and

consider that these two materials belong to the same class from the viewpoint of difficulties of the INS studies of lattice dynamics.

The generalized phonon density-of-states (GDOS) has been measured in natural boron-based MgB_2 . This experiment is described in detail in [9]. Here we mention just the most essential facts. Since the neutron penetration depth in Pu is less than 0.5 mm, the reflection geometry is much better than the transmission one.

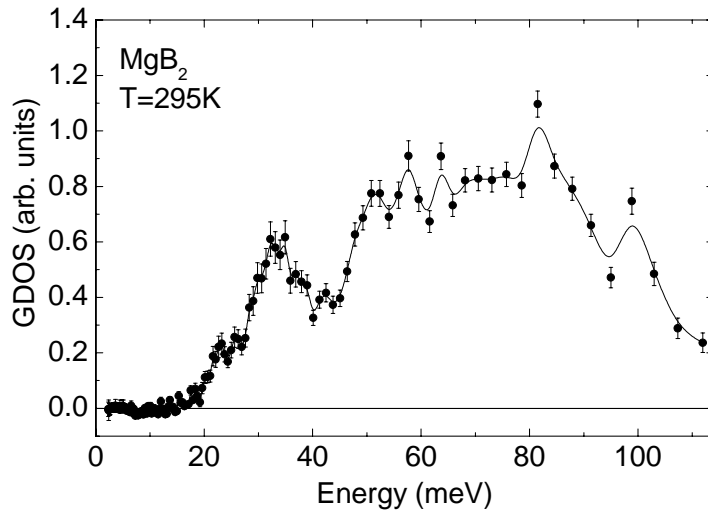


Fig 2: Generalized phonon density-of-states (GDOS) in MgB_2 at $T=295\text{K}$ [9]. The data corrected for the multiphonon scattering, Debye-Waller attenuation and background contributions.

A huge sample area (more than 300 cm^2) was a crucial factor. The inverted geometry time-of-flight spectrometer KDSOG-M (IBR-2, Dubna) was used with a fixed final energy 4.9 meV. The energy of the incoming neutron beam was in the range 5 meV to 120 meV for the phonon spectrum in MgB_2 . Since the outgoing neutron energy was rather small, the experimental conditions were not optimal due to much higher absorptions rates at lower neutron velocities. Nevertheless a reasonable statistics was collected within a few days (Fig. 2). The experimental conditions could be improved by choosing higher final neutron energy for the inverted geometry case (or higher incoming energy in the direct geometry spectrometer case). Another obvious option is moving to a neutron source with much better luminosity than IBR-2

in Dubna and to an instrument with bigger detector blocks and better solid angles compared to KDSOG-M.

We conclude from this study that the difficulties of the INS experiment on ^{239}Pu -based compounds are not so dramatic and such an experiment is conceivable. In particular the phonon density-of-states could be studied in detail within a few days on a conventional neutron source or even a few hours on an advanced neutron source. A time-of-flight spectrometer with a huge detector is the best option for such a measurement. As to the magnetic spectral response study in $\delta\text{-}^{239}\text{Pu}$, we also think that the INS experiment is feasible in principle. A broad energy distribution of the magnetic excitations makes the magnitude of the signal weak, but a better sample transmission at higher energies and negligible phonon scattering (one-phonon and multiphonon) at $E>25\text{ meV}$ makes the things easier.

This work was performed under the auspices of the Russian Federal Agency of Atomic Energy (project "Actinides"). Financial support by the RFBR (grant 05-08—33456-a) is gratefully acknowledged.

- [1] J.C. Lashley *et al.*, Phys. Rev. B **72**, 054416 (2005).
- [2] Los-Alamos Science, ed. by N. Cooper, v. **26** (2000).
- [3] J. Wong *et al.*, Science **301** 1078 (2003).
- [4] R.J. McQueeney *et al.*, Phys. Rev. Lett. **92**, 146401 (2004).
- [5] E. Clementyev *et al.*, Phys. Rev. B **61**, 6189 (2000).
- [6] E. Clementyev, A. Mirmelstein and P. Böni, *to be published* (2006).
- [7] M. Wulff *et al.*, Phys. Rev. B **37**, 5577 (1988).
- [8] S. Kern *et al.*, J. Phys. Cond. Matt. **2**, 1933 (1990).
- [9] E. Clementyev, *et al.*, Eur. Phys. J. B **21**, 465 (2001).

Monte Carlo + Molecular Dynamics simulation of radiation damage evolution and Helium dynamics in Plutonium

V.V. Dremov, P.A. Sapozhnikov, S.I. Samarin, D.G. Modestov, N.E. Chizhkova, G.V. Ionov

Russian Federal Nuclear Centre – Zababakhin Institute of Applied Physics (RFNC-VNIITF)
Snezhinsk, Russia 456770

ABSTRACT

Combined effect of radiation damage and Helium accumulation in Pu metal (as a result of alpha decay) upon thermodynamic and mechanical properties and phase stability is the key questions in the problem of ageing. Atomistic approach to the simulation of these complicated processes is rapidly developing direction of theoretical material science.

The paper presents results obtained in the simulation of damage cascades in self-irradiated unalloyed and gallium-alloyed delta-plutonium. The fast cascade stage was simulated by Monte Carlo method. When the energies of cascade particles became close to the displacement energy, the cascade configuration resulted (coordinates + particle velocities) was transferred to a molecular dynamics (MD) code. The Modified Embedded Atom Model (MEAM) [1,2] was used to describe particle interactions at low energies. Applying combined technique allows 1) to take into account energy loss due to inelastic scattering taking place at high particles energies and to eliminate MEAM shortcomings at small interatomic distances; 2) to track the evolution of the system in time. Problems arising from Monte Carlo binary collision approximation when applying to calculation of cascaded caused by uranium atom have been considered.

Our simulations show that a cascade from the uranium recoil nucleus causes a large energy release into a lattice subsystem within a local region measuring about 20-25 nm; this causes material melting and subsequent recrystallization. Preliminary estimates showed that the energy transferred to the lattice is enough to cause melting in a region which characteristic size reaches 15 nm; the region contains ~200 000 atoms. MD simulations show that lattice heat conductivity reduces the characteristic size of the melting region to ~8-10 nm (~35 000 atoms) in a sample whose initial temperature was 300K. Further dissipation of heat from the melted region results in recrystallization process. The time of full recrystallization was estimated to be ~1ns.

The spatial distribution of point defects in the recrystallized region was obtained. Most of point defects created during a fast stage of the cascade vanish when melting and recrystallizing, residual defects evolve much slower than the nano-second time scale.

MD simulations of the damage cascade evolution have also been carried out in the presence of Helium bubbles ~1-2nm in diameter. The evolution of temperature and density fields in the damaged region and in the vicinity of bubbles has been tracked in the simulations. It was shown that temperature gradients caused by local energy release in the cascades lead to the He bubbles mobility.

To recognize different type of defects and crystal structures the new technique that was called Adaptive Template Analysis (ATA) has been developed. Comparison of ATA with widely used Common Neighbors Analysis and Centro-Symmetry Analysis has been carried out.

1. M. I. Baskes, *Phys. Rev. B*, v. 62 (2000), p. 15532.
2. M. I. Baskes, K. Muralidharan, M. Stan, S. M. Valone, F. J. Cherne, *JOM* 55 (2003), p. 41.

Applicability of Elastic-Plastic Estimations to the Energy of Mixing of Solid Solutions

V.M Elkin, V.N. Mikhaylov, T.Y. Mikhaylova

Russian Federal Nuclear Center – Zababakhin Institute of Applied Physics

P.O. Box 245, Snezhinsk, Chelyabinsk Region Russia 456770

E-mail: v.m.elkin@vniitf.ru

One of the components of free energy of solid solutions is the energy of elastic distortions from the difference in the atomic radii of materials present in an alloy (the size factor). In the theory of solid solutions, the mixing energy associated with elastic distortions is usually estimated using the model of non-coincident spheres in the approximation of continual mechanics and linear isotropic elasticity theory. Though the approximation is very crude, the elastic model gives, in some cases, quite reasonable estimates for the heat of mixing. However, its use causes difficulty if the size factor is large. To decide whether the elastic model is applicable or not requires the direct comparison of calculated and experimental data. This becomes possible with atomic displacements in the vicinity of the atom of the alloying element obtained in EXAFS measurements [1,2].

The paper discusses displacements associated with the size factor which were calculated in elastic and elastic-plastic approximations. We have to consider plastic deformations because stress deviator intensity near the dilatation center exceeds the theoretical yield stress. Two dilatation center models are considered: a single atom of the alloying element and a cluster of 12 neighbor atoms. The second model seems more realistic because the behavior of lattice parameters markedly deviates from Vegard law pointing to a strong interaction between the atom of the alloying element and the surrounding host atoms that was also proved by ab initio calculations [3].

Calculations performed for the δ -phase Pu-Ga alloy show that displacements in the first coordinate sphere obtained with all the above models are much smaller than experimental ones. This disagreement between calculated and experimental data comes from elastic moduli softening near the dilatation center that causes negative pressures in material, and from the strong dependence of elastic moduli on strain.

Thus we have found that simple elastic-plastic estimations of the energy of elastic distortions associated with strong volume collapses are inapplicable to materials with elastic moduli strongly dependent on strain.

[1] L.E. Cox, R. Martinez, J.H. Nickel, S.D. Conradson, and P.G. Allen, Phys.Rev. B 51, 751 (1995)

[2] Ph. Fauer, B. Deslandes, D. Bazin, C. Tailland, R. Doukhan, J.M. Fournier, and Falanga, J. Alloys Comp. 244, 131 (1996)

[3] B. Sadigh, W.G. Wolfer, Phys.Rev. B 72, 205122 (2005)

Enhancement of Localized Magnetism due to Kondo-ions

A. Mirmelstein¹, E. Clementyev¹, G. Lapertot²

¹ RFNC-VNIITF, Snezhinsk, Russia, ² DRFMC/SPSMS/GM, CEA-Grenoble, France

The effect of magnetic rare-earth ions dilution by Ce on the magnetic ordering temperature was investigated for the isostructural intermetallic compounds PrNi and GdNi. According to DC magnetization and AC susceptibility measurements the Curie temperature turns out to be dramatically enhanced in both $\text{Pr}_{1-x}\text{Ce}_x\text{Ni}$ and $\text{Gd}_{1-x}\text{Ce}_x\text{Ni}$ as compared to the reference $\text{Pr}_{1-x}\text{La}_x\text{Ni}$ и $\text{Gd}_{1-x}\text{La}_x\text{Ni}$ systems, respectively. This is a clear evidence of a strong influence of the partially delocalised cerium 4f electrons on the magnetic ordering in the Gd-sublattice.

It is well known that the ground state of rare-earth (RE) based intermetallic compounds forms as a result of a complex interplay of RKKI coupling, Kondo interaction, and the crystal-field potential [1]. The main features of the first two interactions have been intensively studied for decades in many Ce-, Yb- and U-based materials. It is well understood that there is a competition between Kondo- and RKKI interactions since the formation of a Kondo-singlet prevents an exchange coupling of neighboring RE magnetic moments. At the same time, almost nothing is known on how partially delocalized 4f states of a Kondo-ion like Ce affect magnetic ordering phenomena in the RE intermetallics with fully localized magnetic moments.

Thus, the aim of the present paper is to study the effect of magnetic RE ions substitution by Ce on the magnetic ordering temperature for the isostructural intermetallic compounds PrNi and CeNi. These materials, as well as CeNi and LaNi, crystallize in the orthorhombic CrB-type structure (space group *Cmcm*) and show complete solid solubility with respect to the RE/Ce/La substitutions. The samples under study were synthesized by arc melting in argon atmosphere starting from high purity metallic components and then were undergone to the long-term homogenizing annealing in dynamic vacuum. The single-phase character of all the samples was confirmed by X-ray powder diffraction. Magnetic properties (DC magnetization and AC susceptibility) were measured using commercial PPMS instrument (Quantum Design) in a temperature interval 1.8 to 300 K.

GdNi is a simple collinear ferromagnet with a pure spin magnetic moment ($S = 7/2, L = 0, J = 7/2$) and Curie temperature $T_c = 73$ K. PrNi ($S = 1, L = 5, J = 4$) is also a collinear ferromagnet ($T_c = 20.5$ K), but with more complex behavior due to the crystal-field effects and unusual (soft) magnetic dynamics [2]. CeNi is a

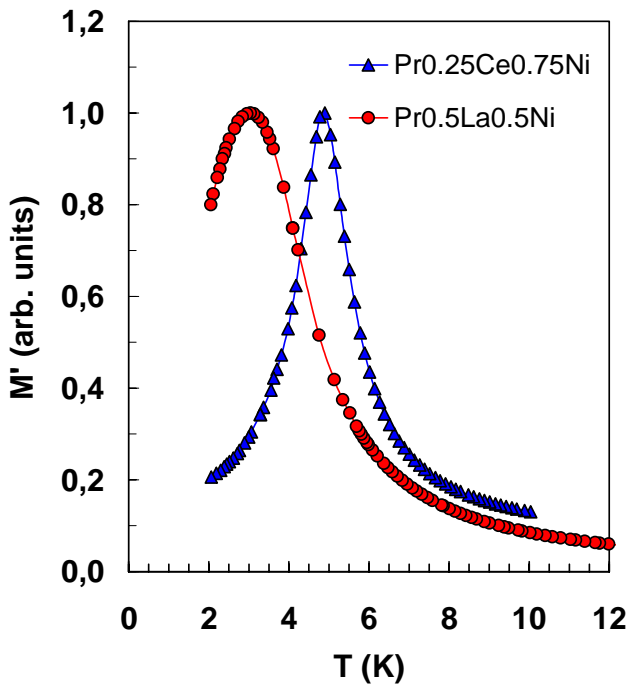


Fig. 1. Real part of the AC susceptibility M' for $\text{Pr}_{0.25}\text{Ce}_{0.75}\text{Ni}$ and $\text{Pr}_{0.5}\text{La}_{0.5}\text{Ni}$. The Curie temperature T_c corresponds to the maximum of the curves.

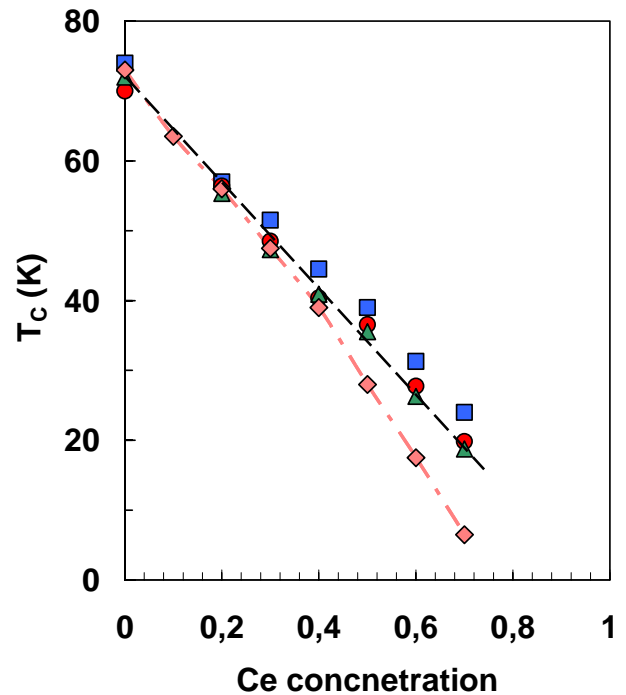


Fig. 2. Dependence of T_c on Ce concentration in $\text{Gd}_{1-x}\text{Ce}_x\text{Ni}$. Squares, paramagnetic Curie temperature θ_p ; circles, T_c determined by the maximum of M' ; triangles, T_c determined as the inflection point of DC magnetization. Rhombs show T_c for $\text{Gd}_{1-x}\text{La}_x\text{Ni}$ according to the AC susceptibility measurements from ref. [4].

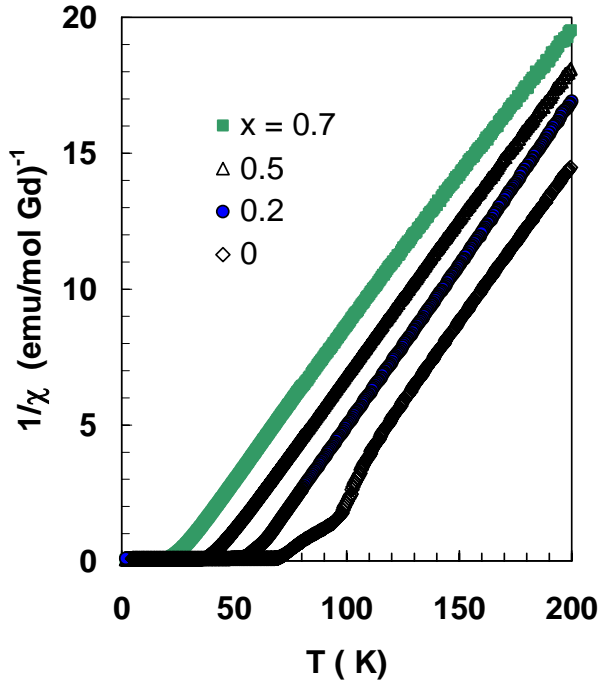


Fig. 3. Normalized (per Gd mol) inverse susceptibility as a function of temperature for $\text{Gd}_{1-x}\text{Ce}_x\text{Ni}$. Parallel character of $1/\chi$ signals that the effective magnetic moment μ_{eff} of Gd ions does not depend on Ce concentration (see text).

developed at least for the Ce concentration $x > 0.5$: the Curie temperature decreases much slower than for the isostructural $\text{Gd}_{1-x}\text{La}_x\text{Ni}$ [4].

For all the $\text{Gd}_{1-x}\text{Ce}_x\text{Ni}$ compositions under study DC magnetic susceptibility $\chi(T)$ at $T > T_c$ can be well described by the Curie-Weiss law (Fig. 3):

$$\chi(T) = N_A N \frac{\mu_B^2 g^2 J(J+1)}{3k_B(T - \theta_p)} = N_A N \frac{\mu_B^2 \mu_{\text{eff}}^2}{3k_B(T - \theta_p)}, \quad (1)$$

where N is the magnetic ion concentration, μ_{eff} is the effective magnetic moment, and θ_p is the paramagnetic Curie temperature. Figure 2 shows that the values of θ_p are in agreement with T_c obtained as the temperature of M' (T) maximum and the inflection point of DC magnetization. The x -independent slope of the $1/\chi$ vs. T lines in Fig. 3 gives the value of $\mu_{\text{eff}} = 8.37$ for all the compositions under study. This value is close to the theoretical one $\mu_{\text{theor}} = 7.94$ ($g = 2$) for free Gd^{3+} ions. Since the CrB-type structure is highly anisotropic, the difference between μ_{eff} and μ_{theor} can be attributed to the effective powder averaged value of $g = 2.11$.

To conclude, the data obtained provide a strong evidence of Ce substitution-induced enhancement of the localized magnetism in (Pr/Ce)Ni and (Gd/Ce)Ni compounds. Most probably, this effect results from the enhancement of the RKKI interaction in RE sublattice mediated by the partially delocalized $4f$ electrons of Ce.

This work was performed under auspices of Russian Federal Agency for Atomic Energy (project "Actinides"). Financial support by RFBR (grant # 05-08-33456-a) is gratefully acknowledged.

References

1. A.C. Hewson, *The Kondo Problem to Heavy Fermions*, Cambridge University Press (1997).
2. E. Clementyev et al., *Physica B* **350** (2004) 83.
3. D. Gignoux, F. Givord and R. Lemaire, *J. Less-Com. Met.* **94** (1983) 165.
4. E. Gratz et al., *JMMM* **54-57** (1986) 459.

classic intermediate valence system with a nonmagnetic ground state (Kondo-singlet) [3]. Due to chemical pressure the Ce $4f$ electrons are more delocalized in $\text{Gd}_{1-x}\text{Ce}_x\text{Ni}$ than in pure CeNi. LaNi behaves as a normal nonmagnetic material since Ni bears no magnetic moment in the RNi series.

Dilution of a RE magnetic sublattice is expected to decrease T_c . Figure 1 demonstrates such an effect for both (Pr/La)Ni and (Pr/Ce)Ni, i.e. for Pr substitution by either nonmagnetic La or Ce ions characterized by the fluctuating $4f$ shell. However, La substitutions result in more strong effect. In fact, T_c drops down to 3.04 K due to replacement of half of the magnetic Pr ions by La. At the same time, $T_c = 4.90$ K in $\text{Pr}_{0.25}\text{Ce}_{0.75}\text{Ni}$, although 3/4 of Pr ions are substituted by Ce.

In order to prove the effect of enhanced localized magnetism to originate mainly from the influence of Ce $4f$ electrons, rather than from the other factors like variation of the crystal-field interaction due to Pr replacement with nonmagnetic La, we measured the magnetic properties of the $\text{Gd}_{1-x}\text{Ce}_x\text{Ni}$ series ($0 < x \leq 0.8$), in which the crystal field effects are absent because of pure spin origin of the Gd magnetic moments. Figure 2 shows the effect of magnetism enhancement in $\text{Gd}_{1-x}\text{Ce}_x\text{Ni}$ to be well

Influence of decay-induced internal stresses on beta-phase nucleation during alpha-beta transformation of unalloyed plutonium under isothermal condition

A. Troshev (VNIITF)

Poster Session

RAS-IMP (Ekaterinburg) Abstracts

The theory of electronic structure and magnetic properties of Pu and Pu alloys

V.I. Anisimov

Institute of Metal Physics, 620041 Ekaterinburg GSP-170, Russia

The key question in understanding plutonium properties is a problem of $5f$ -electrons localization. For the actinides on the right side of Pu in periodic table starting from americium $5f$ -electrons are fully localized while for the left side elements they are itinerant and contribute to the chemical bonding resulting in a much smaller atomic volume. Pu itself can be as in small volume state (α phase) as well as in large volume state (δ phase). Density functional theory calculations describe well small volume phase but in order to reproduce large volume phase a strong spin-polarization of $5f$ -electrons is needed. That is in contradiction with experimental data showing that there are no local magnetic moments of Pu ions. There are two ways to explain the absence of magnetic moments on localized $5f$ electrons. One is Kondo type screening due to the hybridization of $5f$ electrons with s -, p - and d -electrons. This effect can be described in Dynamical mean-field theory calculations. Another explanation come from the taking into account very strong spin-orbit coupling in this material that can lead to the f^6 configuration with a zero value of total magnetic moment. In the talk a review will be given of various attempts to describe electronic structure and magnetic properties of Pu and Pu alloys in *ab-initio* calculations.

Influence of interstitial impurity and vacancy on δ -Pu magnetic state: *ab-initio* investigation

M.A. Korotin*, A.O. Shorikov*, V.I. Anisimov*, V.V. Dryomov†, Ph.A. Sapozhnikov†

*Institute of Metal Physics, 620041 Ekaterinburg GSP-170, Russia

†RFNC-VNII Technical Physics named after acad. E.I. Zababakhin, Snezhinsk, Russia

INTRODUCTION

In the presentation at the *US-Russian Pu Science Workshop* I would like to discuss the ideas and results described in our abstract at the *Pu Futures — The Science 2006* in more details.

For our investigation of the influence of interstitial impurity and vacancy on δ -Pu magnetic state we have used the so-called *LDA+U+SO* band structure calculation method. It is based on the Local Density Approximation (*LDA*) including Coulomb (U) and Spin-Orbit coupling (SO) in a *generalized matrix form*. The *calculated* values of on-site Coulomb (U), exchange (J_H) and spin-orbit coupling constants (λ) for $5f$ -shell of Pu used in *LDA+U+SO* method as input parameters are $U=2.50$ eV, $J_H=0.48$ eV, $\lambda=0.31$ eV. We have demonstrated that while pure Pu is *nonmagnetic*, the defects of Pu crystal such as interstitial impurity and vacancy could be responsible for *weak magnetism* revealing in various experiments.

There are the items for detailed description and discussion below.

EVOLUTION OF DENSITIES OF STATES FOR PURE δ -Pu

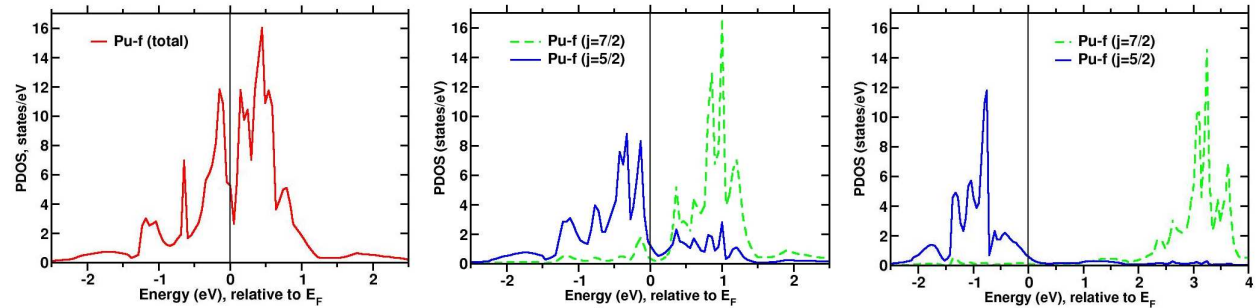


Fig. 1. Projected density of $5f$ -states for pure δ -Pu. **Left panel:** calculated within *LDA*; **middle panel:** calculated within *LDA+SO*; **right panel:** *LDA+U+SO* result.

The origin of nonmagnetic *LDA+U+SO* solution can be traced to the results of standard *LDA+SO* calculations *without* Coulomb correlation correction but *with* spin-orbit coupling taken into account (Fig. 1, middle). The $5f$ -band is split by spin-orbit coupling into well pronounced $f^{5/2}$ and $f^{7/2}$ bands with a separation between their centers ~ 1.5 eV. Comparing Figs.1, middle and right, one can see that taking into account Coulomb correlations via the *LDA+SO+U* correction potential does not change the band structure qualitatively. The only effect is the separation between subbands increases from 1.5 eV to 4 eV that corresponds to the value of $U=2.5$ eV. Another effect of Coulomb interaction is almost pure orbital character of $f^{5/2}$ and $f^{7/2}$ bands in the *LDA+U+SO* calculations comparing with a significant admixture of $f^{5/2}$ orbitals to the nominally $f^{7/2}$ band and vice versa in the *LDA+SO* results. One can say that nonmagnetic $J=0$ solution with $f^{5/2}$ subshell filled with 6 electrons and empty $f^{7/2}$ band is already «preformed» in *LDA+SO*. The role of Coulomb correlations in the *LDA+U+SO* method is to make it more pronounced with a pure orbital nature of the bands and increased energy separation between them.

SEPARATE ACTION OF INTERSTITIAL Pu IMPURITY AND VACANCY

Interstitial impurity and vacancy generate the values and directions of magnetic moments in different ways. As we have investigated for the supercell consisting of 32 Pu atoms originally arranged in the positions of δ phase plus interstitial Pu impurity in one of the octa-holes of FCC lattice (then atomic positions were relaxed in it), the interstitial impurity alone polarizes the $5f$ -shell of neighboring atoms the more, the farther they are (averaged $\mu_{\text{eff}} \sim 0.26 \mu_B/\text{atom}$). The vacancy alone (in the supercell consisting of 8 Pu atoms originally arranged in the positions

of δ phase *minus* one Pu) brings opposite tendency: the nearest neighbors possess maximal moments and the latter decrease with distance (averaged $\mu_{\text{eff}} \sim 0.28 \mu_B/\text{atom}$).

There is one more interesting aspect of the results. Whereas the interstitial impurity alone forms ferrimagnetic order close to AFM A-type inside the supercell, the vacancy alone changes this order to C-type (Fig. 2).

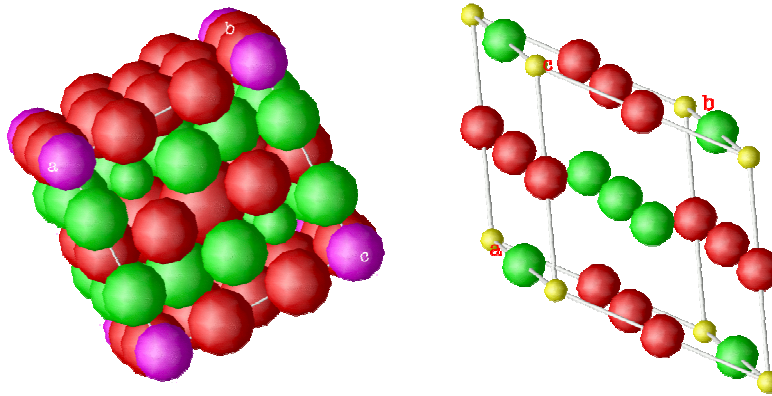


Fig. 2. Calculated magnetic structures for the cases of interstitial Pu impurity (left panel) and vacancy (right panel). **On the left:** magenta balls represent interstitial impurity. The size of ball is proportional to the value of magnetic moment. **On the right:** vacancy are marked by yellow balls. On both panels red and green balls denote different direction of J .

SIMULTANEOUS ACTION OF INTERSTITIAL Pu IMPURITY AND VACANCY

A supercells consisting of 32 Pu atoms originally arranged in the positions of δ phase *plus* interstitial Pu impurity in one of the octa-holes of FCC lattice *plus* vacancy (in fact, minus one Pu) in the first and third coordination spheres of the impurity were constructed. With the use of molecular dynamics Modified Embedded Atom Model (MEAM), the atomic positions were relaxed inside this supercell also. Calculated magnetic structures are presented in Fig. 3. Acting together, two types of defects produce non-collinear magnetic structures shown in Fig. 3 due to the competition of their influences. As to the values of magnetic moments, two types of defects compensate each other more or less, providing weak magnetism (averaged $\mu_{\text{eff}} \sim 0.18 \mu_B/\text{atom}$) of defect plutonium.

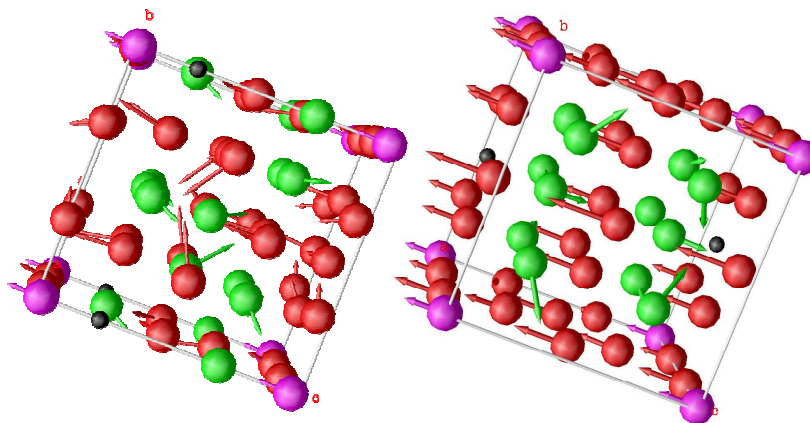


Fig.3. Calculated magnetic structure for Pu supercell with interstitial atom (magenta balls) and vacancy (black balls) close (**left panel**) and far (**right panel**) from each other. Arrows show directions of J , green and red colours correspond to different signs of J_z component. Length of arrows is proportional to μ_{eff} .

CONCLUSIONS

Basing on the $LDA+U+SO$ *ab-initio* calculations we have demonstrated that while pure Pu is nonmagnetic, the defects of Pu crystal such as interstitial impurity and vacancy could be responsible for weak magnetism revealing in various experiments. The calculated value of effective paramagnetic moment is in reasonable agreement with experimental estimates.

M.A.K. acknowledges Russian Science Support Foundation.

Low-frequency spin dynamics of f electrons probed by ^{69}Ga in $\text{Pu}_{0.95}\text{Ga}_{0.05}$ alloy

Yu. Piskunov*, S. Verkhovskii*, K. Mikhalev*, V. Ogloblichev*, A. Buzlukov*, V. Arkhipov*, Yu. Zouev[†], S. Lekomtsev[†], and I. Svyatov[†]

*Institute of Metal Physics, Ural Branch of Russian Academy of Sciences, Ekaterinburg, Russian Federation (piskunov@imp.uran.ru)

[†]Russian Federal Nuclear Center - Institute of Technical Physics, Snezhinsk, Russian Federation

The degree of itinerancy for f electrons in δ -Pu is a problem of real challenge in the fundamental physics of actinides. The very narrow ($\Delta W \sim 700$ K) peak, observed in density of states near the Fermi energy¹, the large value of the Sommerfeld coefficient ($\gamma_{\text{el}} \approx 60 \text{ mJ K}^{-2} \text{ mol}^{-1}$)² indicate, that an effective mass of carriers in conducting band is greatly increased at low temperature in this material. In addition, an abnormal temperature dependence of static spin susceptibility, displayed by ^{69}Ga NMR shift³, and magnetic instability, arisen due to self-damage in δ -Pu alloy at low temperature⁴, suggest to consider this material approaching in electronic properties to the heavy fermion compounds.

We report on the f electron spin dynamics probed by the ^{69}Ga nuclear spin-lattice relaxation time (T_1) in $\text{Pu}_{0.95}\text{Ga}_{0.05}$ alloy (δ -Pu phase). The measurements were performed in magnetic field 9.4 T and the temperature range (10 - 650) K at the very same sample, which for spin contribution to the ^{69}Ga NMR shift (K_s) and static spin susceptibility (χ_s) were discussed in Ref.3. There was shown, that $K_s(T)$ and $T_1(T)$ are controlled correspondingly by static and fluctuating in time parts of local magnetic field arisen at nonmagnetic gallium due to the spin polarization transferred from the f electrons shell of the more magnetic Pu-neighbors.

- Above 200 K the temperature dependent part of the Knight shift tracks the bulk susceptibility $\chi(T)$, following the Curie-Weiss law $K_s(T) \sim (T + \theta_{K_s})^{-1}$ with $\theta_{K_s} = 280(40)$ K, as seen in Fig.1a. Assuming the scenario of completely itinerant f electrons, we should expect the temperature dependence of the product $(T_1 T) \sim K_s^{-2}$, that predicts more steeper rise with T of $(T_1 T)$ than it follows from the experimental data set shown in Fig.1b. The corresponding power-law fit curve $(T_1 T) \sim (T + \theta_{T_1})^{1.5(1)}$ with $\theta_{T_1} = 255(20)$ K is mapped by red color in Fig.1b.

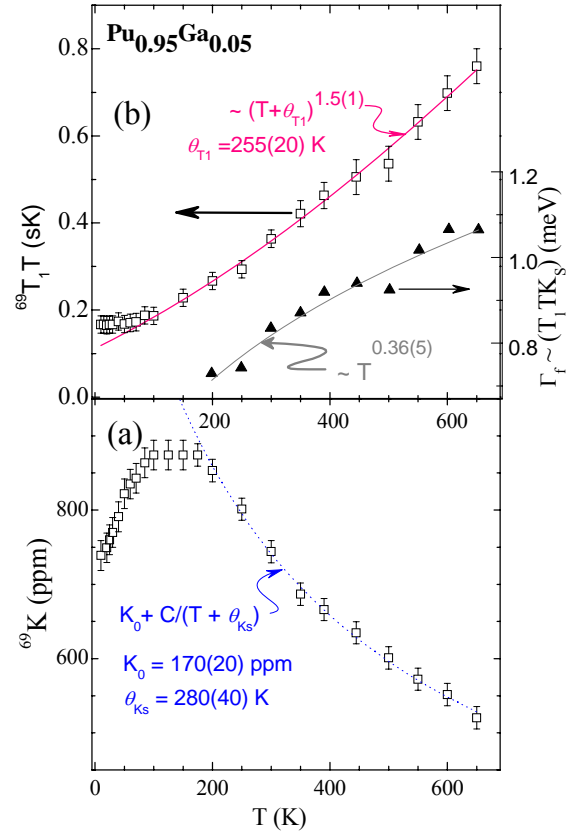


Fig. 1. ^{69}Ga NMR shift (a), the product $^{69}T_1 T$ (b), and Γ_f vs T in $\text{Pu}_{0.95}\text{Ga}_{0.05}$.

- In the more general *case of partially localized behavior of f electrons* the nuclear spin-lattice relaxation rate is defined usually in terms of the q-weighted imaginary part of the dynamic spin susceptibility $\chi''(\mathbf{q}, \omega \approx \omega_{\text{NMR}})$:

$$(T_1 T)^{-1} \sim \sum_{\mathbf{q}} H_f^2(\mathbf{q}) \chi''(\mathbf{q}, \omega_{\text{NMR}}) / \omega_{\text{NMR}}. \quad (1)$$

Here $H_f(\mathbf{q})$ is a hyperfine coupling form-factor, determining hyperfine magnetic field at the Ga nuclei from 5f electrons of Pu. At high temperature range we can ignore both the spin correlations among *f* electrons and the q-dependence of χ'' . Then the expression (1) can be reduced to the following proportionality: $(T_1 T)^{-1} \sim z H_f^2 \chi_f(T) / \Gamma_f(T)$, where, *z* is a number the nearest neighbor of Pu around ^{69}Ga , $\chi_f(T) = \mu_B K_s(T) / z H_f$ is a static spin susceptibility of *f* electrons. So that for independently 3D-fluctuating moments coupled through conducting electrons the characteristic energy of *f* spin fluctuations $\Gamma_f(T)$ follows to the NMR product $(T_1 T K_s)$. The variation with T of $\Gamma_f(T)$ in the $\text{Pu}_{0.95}\text{Ga}_{0.05}$ alloy is shown by up-triangles in Fig1.b, which for the power-law fit $\Gamma_f(T) \sim T^{0.36(5)}$ is close to the T-dependence of $\Gamma_f(T) \sim T^{0.5}$, predicted by Cox et al.⁵ for 3D-Kondo systems at high temperature.

The temperature dependence of nuclear spin relaxation at $T > 100$ K is close to the observed in nonmagnetic Kondo lattice, where the localized electron spins fluctuate independently each other without any macroscopic coherence.

- At low $T < 100$ K the product $(T_1 T)$ becomes independent of temperature, signaling to drastic changes in the regime of spin fluctuations for *f* electrons in the δ -Pu alloy. As usually the relation $(T_1 T) \approx \text{constant}$ is considered as a signature of the Fermi-liquid state for electron in metallic compounds. At $T \sim 10$ K the product $(T_1 T) = 0.18(2)$ sK leads to an estimate of the effective mass of carriers $m^* = 25(3) m_e$, that is approximately twice less of the estimate, following from the Sommerfeld coefficient in the δ - $\text{Pu}_{0.95}\text{Al}_{0.05}$ alloy².

Acknowledgments

The work is supported by the Russian Foundation for Basic Researches (Gr. No 06-02-16130).

¹ A.J. Arko et al., Phys. Rev. B **62**, 1773 (2000).

² J. Lashley et al., Phys. Rev. Letters **91**, 205901 (2003)

³ Yu. Piskunov, et al., Phys. Rev. B **71**, 174410 (2005) ; JETP Lett. **82**, 139 (2005).

⁴ M. Fluss et al., in Abstracts of the V Int. Workshop "Fundamental Pu Properties", Snezhinsk, 2005.

⁵ D.L. Cox et al., J. Appl. Phys. **57**, 3166 (1985).

Poster Session

LANL (Los Alamos) Abstracts

Phase-field Modeling of Coring Structure Evolution and Ga Homogenization Kinetics in Pu-Ga Alloys

S. Y. Hu* , M. Baskes and M. Stan

MST-8, Los Alamos National Laboratory, Los Alamos, NM 78545

During the casting of Pu-Ga alloys, the huge difference of Ga diffusivity in δ and γ phases results in the formation of coring structures which consist of Ga-rich cores with Ga poor edges. On the other hand, the elastic interaction among different oriented δ grains and diffusive Ga might lead to an inhomogeneous diffusion and δ grain growth. In this work, phase-field approach has been used for modeling the coring structure evolution and Ga homogenization kinetics in three dimensions. We assume that the transition from δ (bcc) to γ (fcc) follows the Bain distortion. The chemical free energy is constructed according to the phase diagram. The effect of diffusivity inhomogeneity, internal stresses, anisotropy of interfacial energy and cooling rate on the coring structure evolution is systematically studied. Fig.1 presents the coring structures obtained with and without the effect of internal stresses on the coring structure evolution in two dimensions. The color denotes Ga composition, Red means higher Ga composition while Blue lower Ga composition. The letters “A” and “B” denote two different oriented δ grains. The results demonstrate that the internal stresses speed up the growth in the a-direction, but slow down the growth in the c-direction to minimize the elastic energy, leading to the elongation of the grains as seen in experiments.

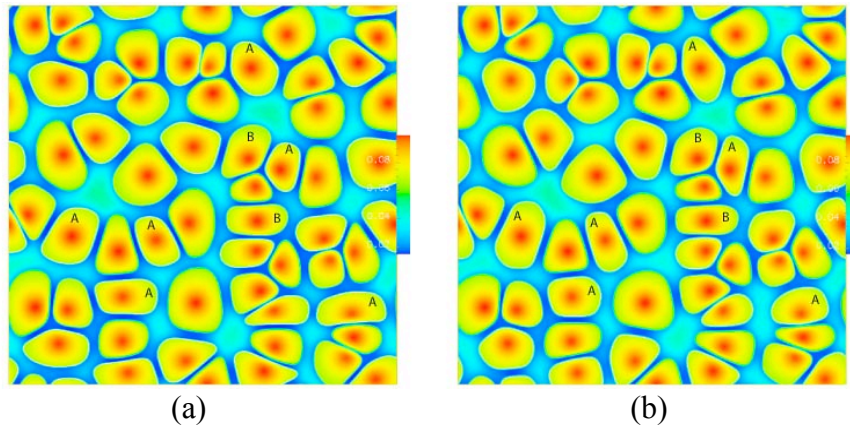


Fig 1: Effect of internal stresses on multi-particle growth in 2D, (a) without internal stresses and (b) with internal stresses

Acknowledgement: This work was supported at Los Alamos National Laboratory by the US Department of Energy under contract W-7405-ENG-36.

STRUCTURE/PROPERTY RELATIONSHIPS OF URANIUM 6WT% NIOBIUM AS A FUNCTION OF TEMPERATURE, STRAIN RATE AND AGING

C.M. Cady, G.T. Gray III, R.S. Hixson, S.R. Chen, D.R. Korzekwa, R.J. McCabe, and M.F. Lopez

Los Alamos National Laboratory, Los Alamos, New Mexico 87545 USA

A rigorous experimentation and validation program is being undertaken to create constitutive models that elucidates the fundamental mechanisms controlling plasticity in Uranium-6 wt.% Niobium (U-6Nb). The model should be able accurately predict high-strain-rate large-strain plasticity, damage evolution and failure by capturing: 1) the mechanical response of a material as a function of strain rate and temperature, and 2) an understanding of the operative deformation mechanisms that must be described in order to build physically-based constitutive models. The stress-strain response of U-6Nb has been studied as a function of temperature, strain-rate, and thermal aging. It was studied in a solution-treated and quenched (ST/Q) and in a solution-treated, quenched and thermally aged at 473K for 2 hours condition. The constitutive behavior was evaluated over the range of strain rates from quasi-static (0.001 sec^{-1}) to dynamic ($\sim 2000 \text{ sec}^{-1}$) and temperatures ranging from 77 to 773K. The constitutive properties were quantified utilizing screw-driven and servo-hydraulic test frames in compression for the quasi-static and intermediate-rate testing and a compressive split-Hopkinson Pressure Bar (SHPB) for the dynamic testing. The yield stress of U-6Nb alloys was found to exhibit pronounced temperature sensitivity but little strain rate sensitivity. The strain hardening rate is seen to be less sensitive to strain rate and temperature beyond plastic strains of 0.10.

LA-UR-06-3923

The Characterization of Shear Deformation and Shock Damage in U6Nb

E. Cerreta, G.T. Gray III, P. J. Maudlin, C.A. Bronkhorst, R. J. McCabe, C.P. Trujillo, C.M. Cady,
and A.M. Kelly

The damage evolution and the failure response of U6Nb has been linked to shear localization and cracking during high rate loading. However, the details of porosity, shear banding, and cracking during deformation are not always well understood and the role of stored work on the mechanical response of U6Nb under high strain rates is unclear, particularly in relation to defect evolution. Here the shock induced microstructure is characterized in U6Nb plate material. The influence of stored work in the form of cold rolling and preshock on shear deformation is probed through a series of high strain rate tophat experiments and the influence of dynamic strain rate and temperature on the mechanical response in shear, shear band formation, and damage evolution in U6Nb is characterized.

PuCoGa5: Bridging the Gap between Heavy Fermion and High-Temperature Superconductivity

Nicholas Curro
Condensed Matter and Thermal Physics
Los Alamos National Laboratory

We report nuclear magnetic resonance (NMR) data in the new heavy fermion superconductor PuCoGa5 ($T_c = 18.5\text{K}$) in the normal and superconducting states. Measurements of the Knight shift and the nuclear spin lattice relaxation rate in the superconducting state reveal a spin singlet order parameter with d-wave symmetry. In the normal state, the spin lattice relaxation rate is driven by antiferromagnetic correlations, and scales with T_c as in other heavy fermion superconductors, as well as the high temperature superconductor YBa₂Cu₃O₇.

Temperature and time-dependence of the elastic moduli of Pu and Pu-Ga alloys

Albert Migliori, D. Miller, D. Dooley, M. Ramos, R.J. Byars, J.B. Betts, I Mihut*

*Los Alamos National Laboratory, Los Alamos, New Mexico 87545

INTRODUCTION

We measured the elastic moduli of Pu and Pu-Ga alloys with three goals. They are 1) Provide accurate elastic moduli, 2) provide accurate temperature dependence, and 3) Measure the relative changes with time. We summarize here results for the time dependences with conclusions and results important to LANL and LLNL programs.

Fig. 1 shows an example of an RUS system for use with Pu and Pu-Ga alloys. A complete description of this system and a review of RUS are described by Migliori et al.[1] We have measured Pu, Pu-Ga alloys and an Accelerated-Aging Program (AAP) alloy at ambient and cryogenic temperatures. The AAP alloy “ages” at a rate 16.5 times that of normal ^{239}Pu and it was “made” on 15 May 2002. All measurements presented were performed on fine-grained polycrystal, accurately-polished RPR's of known composition. It is expected that some formation of mechanically-induced alpha-Pu has occurred in delta-Pu specimens, but because all samples are at least as large as a 2mm cube, minimal errors in absolute moduli are calculated from this effect.

TIME DEPENDENCE OF ELASTIC MODULI OF PU AND PU-GA ALLOYS

To understand the variation of the elastic moduli with time in Pu one must keep in mind several effects. These are: 1) Pu-Ga alloys are not thermodynamically stable at ambient temperature. 2) As ^{239}Pu decays radioactively, interstitial-dislocation pairs are produced, about 2200/decay. 3) Decay products include He and metals that are not Pu, and so can change physical properties. A few key referents include: 1) from radioactive decay, 3.16×10^{-9} of the Pu atoms present in a specimen decay per hour, 2) 6.9×10^{-6} Frenkel pairs/hour/atom are produced, 3) From measurements of 3.3 at. % Ga and the 3.9 at. % Ga samples, the maximum long term fractional rate of change of the bulk modulus is of order $9 \times 10^{-7}/\text{h}$, 4) The elastic moduli change at a rate much higher than that of e.g. the density or Frenkel pair retention rate. Thus from the raw Frenkel pair production rate, we can estimate that the elastic moduli change at a fractional rate of order $7 \times 10^{-5}/\text{h}$. These rates are limiting associated with radioactive decay and very low temperature. Any rate substantially different from these must be associated with other physical effects.

It is important to note that the effects seen are much smaller than the error bars for measurements presented above. This is because the precision of RUS for Pu specimens is of order 5 parts in 10^7 , but absolute accuracy is limited by errors in the measured size of specimens, of order several tenths of a percent.

Measurements were made using a very-high-precision temperature control system that held temperatures to within a few mK over many days. Good temperature control is crucial because of the strong temperature dependence of the elastic moduli of all samples.

In Fig. 2 we show the time dependence of the moduli of alpha Pu and Pu 2.36 at. % Ga. We can extract an important time scale from these measurements. Note that at 10K where Frenkel pairs are expected, from other studies, to be approximately fully retained, with less than a few tens of percent immediately annealing out, we find that delta Pu shear modulus *decreases* at a fractional

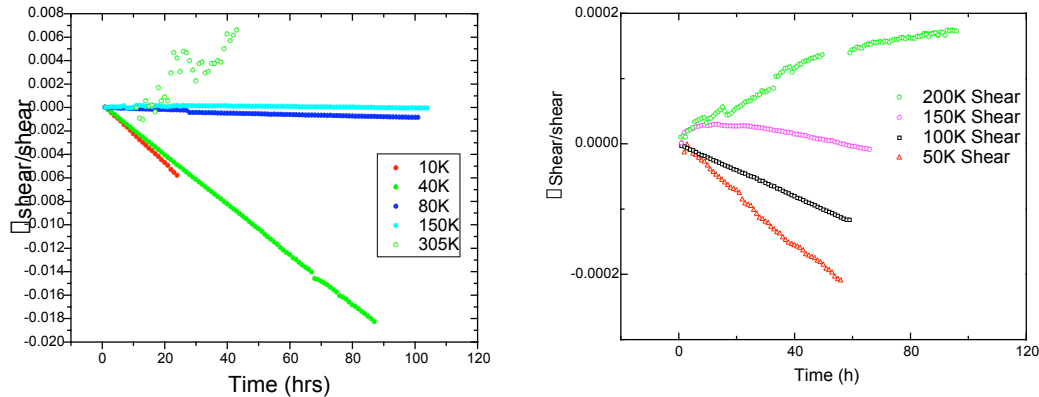


Figure 2. Left: The normalized shear modulus change for alpha Pu versus time and temperature. Right: The normalized shear modulus change for Pu 2.36 at. % Ga versus time and temperature.

rate of about $4 \times 10^{-5}/\text{h}$ and that the modulus of alpha Pu decreases at a higher rate, about $20 \times 10^{-5}/\text{h}$. The differences are not surprising in light of the differing responses of alpha and delta Pu to radiation damage. *We conclude unambiguously that radiation damage reduces the elastic moduli of Pu alloys.* Thus the time variation of these samples is strictly associated with Frenkel pair production, and *because both alpha and delta change approximately similarly, we can rule out any effects from thermodynamic reversion of the phases predicted by the Russian phase diagram.*

The time scales associated with thermal equilibration of Frenkel pairs can now be determined. Using a relaxation model, our measured difference in bulk modulus of normal and AAP Pu (about 52.3-51.3=2%), the difference in the rate of Frenkel pair production between AAP and normal Pu (a factor of 16) and, and the approximate measured rates of change near room temperature convoluted with the maximum estimated total change ($\Delta B_0/B_{aging}=15$ years), we can self-consistently find the Frenkel pair main relaxation rate from

Where we find $B_{aging}=0.16\%$, and $\tau=8$ days. Thus in of order a month, the elastic moduli stabilize, and any further time dependences must be associated primarily with He and U production.

ACKNOWLEDGEMENTS

This work was supported by the State of Florida, the NNSA, and the LANL laboratory directed research and development program and Enhanced Surveillance.

The α - α' Transformation in Aged Pu-Ga alloys

J.N. Mitchell, D.S. Schwartz, and T.E. Mitchell

Los Alamos National Laboratory, Los Alamos NM 87545 USA

The martensitic $\alpha \rightarrow \alpha'$ transformation in Pu-Ga alloys has several fascinating characteristics, including a >20% volume reduction, a reversion hysteresis of up to 200 °C, and an apparent maximum transformation of about 25 vol. %. We are studying this transformation in a variety of materials, including aged samples, and will discuss the differences that we have observed in transformation behavior. We will emphasize results that reveal the differences between as-aged and thermally reset samples and propose mechanisms that may explain these differences.

Aging and Phase Stability in Delta-Stabilized Pu: Local and Long-Range Order

L. Morales

Superconductivity and Magnetism in PuCoGa₅ and Related Materials

J. D. Thompson, N. J. Curro, Tuson Park, and J. L. Sarrao

Los Alamos National Laboratory, Los Alamos, NM 87545 USA

Superconductivity in actinide-bearing compounds has served as a tool for guiding an interpretation of the role that 5f-electrons play in determining physical properties. Likewise, an interpretation of the mechanism of superconductivity must be consistent with what is known about the normal-state properties of these compounds. PuCoGa₅, the first Pu-based superconductor [1], exemplifies these complementary approaches to revealing the nature of plutonium's 5f-electrons in this compound. Its superconducting transition temperature T_c of 18.5K is nearly an order of magnitude higher than that of any previously known 5f-electron material but comparable to T_c 's found in some transition-metal intermetallic compounds. Unlike these other intermetallics whose superconductivity is conventional, i.e., mediated by an attractive electron-phonon interaction, the uniform magnetic susceptibility of PuCoGa₅ is Curie-Weiss-like, with an effective moment expected for a nearly localized 5f⁵ configuration. Because the presence of a local moment is detrimental to conventional superconductivity, this suggests the possibility that superconductivity of PuCoGa₅ is unconventional, e.g. mediated by a magnetic interaction, which is the case in strongly correlated electron materials, such as the high- T_c cuprates and heavy-fermion systems based on Ce or U. This possibility is borne out by NMR measurements [2,3] that find a power-law dependence of the nuclear-spin relaxation rate $1/T_1$ in the superconducting state of PuCoGa₅ as well as in the isostructural superconductor [4] PuRhGa₅ with $T_c=8.5$ K. Further, $1/T_1$ in the normal states of these materials also is unconventional and consistent with nuclear-spin relaxation being dominated above T_c by the presence of 5f-electron spin fluctuations. Together, these experiments lead to a picture of superconductivity mediated by magnetic fluctuations associated with Pu's 5f electrons whose characteristic spin fluctuation rate is set by hybridization with ligand electrons. This interpretation also is consistent with the suppression of T_c with self-radiation damage, the temperature dependence of electrical resistivity, the large value of a magnetic field required to suppress superconductivity, and an enhanced Sommerfeld coefficient of specific heat that are found in these Pu superconductors.

Hybridization of 5f and ligand electrons not only sets the characteristic energy scale for spin fluctuations but also the bandwidth of electronic states at the Fermi energy E_F . In a simple approximation, the inverse of the bandwidth is proportional to the density of electronic states at E_F measured by the Sommerfeld specific heat coefficient. The superconducting transition temperatures of Ce- and U-based heavy-fermion compounds, the high- T_c cuprates and these Pu superconductors appear to have a common linear dependence on the energy scale set by hybridization.² The T_c 's of PuCoGa₅ and PuRhGa₅ are intermediate to those of these two other families of superconductors, implying that the 5f electrons of the Pu superconductors are not as localized as the f-electrons in heavy-fermion systems but more localized than the d-electrons of the cuprates. This is the same correlation expected on the basis of the spatial extend of the relevant f- or d-electrons and equivalently of their effective bandwidth or Sommerfeld

coefficient. Extending this picture to elemental Pu suggests that its 5f electrons are strongly hybridized with band electrons, preventing it from being either superconducting or magnetic.

Besides superconductivity, are there other surprises waiting to be found in PuCoGa₅ or PuRhGa₅? The answer is almost certainly yes. One possibility comes from a comparison with the isostructural heavy-fermion compounds CeCoIn₅ and CeRhIn₅ in which hybridization can be tuned by readily accessible pressures and magnetic fields. Though CeCoIn₅ is superconducting at atmospheric pressure, CeRhIn₅ is antiferromagnetic but becomes superconducting with applied pressure. Imposing a magnetic field on CeRhIn₅ in its superconducting state induces magnetic order that is hidden by superconductivity in the absence of a field.[5] Various theoretical models have been proposed for how this can happen, but the observation of field-induced magnetic order coexisting with superconductivity remains unresolved. The unusual temperature dependence of the nuclear-spin relaxation rate in PuRhGa₅ is strikingly similar to that of CeRhIn₅ under pressure, suggesting that the relative f-electron hybridization is comparable in both materials which also is true for PuCoGa₅ and CeCoIn₅. From this comparison, it seems worthwhile to search for field-induced magnetism in PuRhGa₅, which, if found, would allow a new approach to probing the nature of plutonium's 5f-electrons and its the evolution with field tuning.

Work at Los Alamos was performed under the auspices of the U.S. Department of Energy, Office of Science.

- [1] J. L. Sarrao et al., Nature **420**, 297 (2002).
- [2] N. J. Curro et al., Nature **434**, 622 (2005).
- [3] H. Sakai et al., J. Phys. Soc. Jpn. **74**, 1710 (2005).
- [4] F. Wastin et al., J. Phys. Condens. Mat. **15**, s2279 (2003).
- [5] Tuson Park et al., Nature **440**, 65 (2006).

Multi-Scale Modeling of Aging in Plutonium Alloys

S. M. Valone, M. I. Baskes, R. G. Hoagland, and B. P. Uberuaga

Materials Science and Technology Division, Los Alamos National Laboratory, Los Alamos, New Mexico 87545

Modeling the evolution of plutonium-gallium (Pu-Ga) alloys is extremely important for understanding these actinide materials [1] that age through spontaneous fission of the Pu that results in production of uranium and helium (He) atoms, as well as cascade damage that starts as point defects and small clusters of interstitials and vacancies. All types of defects evolve into larger scale features, and, in particular, the He atoms gradually accumulate into bubbles. The damage evolution process and changes in strength as a result of these defects [2] are modeled at several length-scales.

At the atomic scale, the modified embedded atom method (MEAM) formalism [3, 4] has been applied to Pu [5], Ga [6], Pu-Ga alloys [7], and the Pu-Ga-He system [8]. Many of the atomic level interactions are estimated from electronic structure calculations. From the atomistic model we are able to directly simulate the cascades in the material via molecular dynamics [9]. The damage left over from the rapid quenching from the cascade is evolved through accelerated molecular dynamics [10]. These simulations reveal that small vacancy clusters (6-40 vacancies) in Pu can transform to stacking fault tetrahedra. The effects of a few He atoms on vacancy clusters and their migration is also being studied. The atomistic model also provides an a view of the alloys and He bubbles at the scale of tens of nanometers. The local structure around He bubbles can be effected by temperature, internal bubble pressure, and local Ga concentration. Finally this model provides a means of estimating the pinning strength of a dislocation to He bubbles, which involves length-scales on the order of hundreds of nanometers . The strength change estimate can be used, for example, in an Orowan equation for the flow stress of the aging material. Changes in pinning sources are occurring at the sub-grain level.

This work was performed at Los Alamos National Laboratory under the auspices of the U. S. Department of Energy, under contract No. W-7405-ENG-36.

-
- [1] A. J. Schwartz, M. G. Wall, T. G. Zocco, and W. G. Wolfer, *Phil. Mag.* **85**, 479 (2005).
 - [2] A. Arsenlis, W. G. Wolfer, and A. J. Schwartz, *J. Nucl. Mater.* 336 (2005) 31.
 - [3] M. I. Baskes, *Phys. Rev. B* **46**, 2727 (1992).
 - [4] M. I. Baskes, *Mater. Sci. Eng. A* **261**, 165 (1999).
 - [5] M. I. Baskes, *Phys. Rev. B* **62**, 15532 (2000).
 - [6] M. I. Baskes, S. P. Chen, and F. J. Cherne, *Phys. Rev. B* **66**, 104 (2002).
 - [7] M. I. Baskes, K. Muralidharan, M. Stan, S. M. Valone, and F. J. Cherne, *JOM* 55, 41 (2003).
 - [8] S. M. Valone, M. I. Baskes, and R. L. Martin, *Phys. Rev. B* (2006), in press.
 - [9] S. M. Valone, M. I. Baskes, M. Stan, T. E. Mitchell, A. C. Lawson, and K. E. Sickafus, *J. Nucl. Mater.* **324**, 41 (2004).
 - [10] A. F. Voter, *Phys. Rev. B* **57**, 13985 (1998).

Livermore, July 14-15

Factors Contributing to the Dynamic Behavior of Metals

A. Zubelewicz

Los Alamos National Laboratory, Los Alamos, NM 87545, U.S.A

Metals subjected to extreme loading rates exhibit properties characteristic of a thermodynamically open system. The openness manifests itself through an exchange of energy that is carried by dislocations traveling long distances with a nearly sonic velocity. Since such phenomena are rarely observed in solids, mean-field theories of nonlinear continuum dynamics are considered sufficient in representing the behavior of metals. We will show that the classic theories are too restrictive when describing metal behavior at extreme loading rates. Our dynamic defect structure (DDS) model predicts that various metals subjected to extreme loading rates experience a strong mesoscale excitation leading to an entrapment of kinetic energy. The behavior has already been observed in tantalum and iron, where line visar measurements confirm existence of a highly perturbed profile of the free surface velocity. While a significant portion of the entrapped energy is converted into heat, the remaining part supports a rearrangement of the material's internal structure and causes fluctuations in the fields of velocity, strains, and stresses. The DDS theory explains a remarkable increase in the plastic hardening rate observed in copper, iron, nickel, aluminum, titanium, and steel at strain rates greater than 10^3 s^{-1} . Furthermore, DDS confirms findings that metals subjected to extreme loading rates dissipate energy in a non-uniform manner. This process is coupled with the formation of localized shear and coarse slip bands. We present capabilities of the DDS theory by incorporating it into a modified power-law constitutive model.

Poster Session

LLNL (Livermore) Abstracts

Molecular dynamics simulations of the interaction between shock waves and high-symmetry intergranular boundaries

Vladimir Dremov¹, Philipp Sapozhnikov¹ and E.M. Bringa^{2*}

¹*Russian Federal Nuclear Center - Institute of Technical Physics,*

Snezhinsk, 456770 Chelyabinsk reg., Russia

²*Lawrence Livermore National Laboratory, Livermore, CA 94551, USA*

**Presenting author*

The paper presents results of the molecular dynamics simulation on the interaction of a shock wave with a highly-symmetric grain boundary in copper. Our calculations were done for five slopes of the boundary (110) \square 5 to the shock front and for two levels of loading: above the Hugoniot elastic limit (HEL) but below the critical level at which the homogeneous dislocation production occurs (Homo) and above that critical level. Shock-induced defects and their role in shear stress relaxation have been analyzed. It has been shown that there are two competing shear stress relaxation mechanisms as a result of the grain boundary shock interaction. Calculations of the temperature evolution in the vicinity of the grain boundary make evidence for the possibility of local melting far below the intersection of the Hugoniot and the melting line.

This work was performed under the auspices of the U.S. Department of Energy by University of California, Lawrence Livermore National Laboratory under contract of No.W-7405-Eng-48, LDRD 04-ERD-021.

Spectroscopic and Physical Measurements of Aging in Plutonium

B.W. Chung, J.G. Tobin, S.R. Thompson, and B.B. Ebbinghaus

Lawrence Livermore National Laboratory, P.O. Box 808, Livermore, CA, 94551

Plutonium, because of its radioactive nature, ages from the “inside out” by means of self-irradiation damage and thus produces Frankel-type defects and defect clusters. The defects resulting from the residual lattice damage and helium in-growth could result in microstructural, electronic, and physical property changes. This paper presents volume, density, and electronic property change observed from both naturally and accelerated aged plutonium alloys. Accelerated alloys are plutonium alloys with a fraction of Pu-238 to accelerate the aging process by 18 times the normal rate. After fifty-five equivalent years of aging on accelerated alloys, the samples at 35°C have swelled in volume by 0.15% and now exhibit a near linear volume increase due to helium in-growth. The resonant photoemission measurements on ten years old delta plutonium shows strong enhancement of the valence band compared to a fresh plutonium alloy. This enhancement is attributed to increased localization induced by self-irradiation damage.

This work was performed under the auspices of the U. S. Department of Energy by the University of California, Lawrence Livermore National Laboratory under Contract No. W-7405-Eng-48

Dynamic Strength of Metals in Shock Deformation

Alison Kubota, David B. Reisman, and Wilhelm G. Wolfer

Lawrence Livermore National Laboratory, Livermore, California, 94550-9234, USA

The Hugoniot and critical shear strength of shock-compressed metals can be obtained directly from molecular dynamics simulations without recourse to surface velocity profiles and their analyses. Results from simulations in aluminum containing an initial distribution of microscopic defects are shown to agree with experimental results.

We give a brief account of mapping results from MD simulations on a continuum description for the spatial and temporal distributions of all the thermodynamic variables: temperature, stresses and their rates, strains and their rates, and derivative parameters such as pressure, density, von Mises stress, and plastic strain and strain rates. With this information, it is then possible to directly relate pressure to density and temperature, and thereby construct Hugoniot curves of solid and liquid materials, without recourse to the Rankine-Hugoniot relationships. We can also directly determine the dynamic strength of materials from the spatial distribution of the von Mises stress.

Self-Damage and Magnetic Susceptibility in Pu and Pu alloys as a Probe of the 5f electrons

S.K. McCall, M.J. Fluss, B.W. Chung, G.F. Chapline, M.W. McElfresh, and D.J. Jackson
Lawrence Livermore National Laboratory, Livermore CA 94550 USA

Abstract

The 5f-electrons of both α -Pu and δ -Pu occupy a narrow f -band as indicated by the large magnitudes of both the electronic specific heat and Pauli (temperature independent) magnetic susceptibility. While some theoretical models of Pu accurately predict the energy-volume relationship of the various Pu phases, they require non-vanishing magnetic moments, yet there are no experimental measurements indicating any sort of localized moments in the “pure” metal[1, 2]. However the narrow f -band suggests that Pu is nearly magnetic, and should display evidence of magnetic moments given an appropriate perturbation.

The Hill conjecture postulates that within the actinides magnetism or its absence is determined primarily by the actinide separation[3]. For plutonium compounds, a separation greater than 3.4Å should produce magnetic moments. Indeed, this is observed for fluorite structured PuH₂, where the Pu atoms retain an FCC structure akin to the δ -phase, with the hydrogen atoms effectively acting as spacers to stretch the Pu-Pu distance to 3.79Å, leading to local moments ($\sim 1\mu_B$ /Pu) that antiferromagnetically order at 30K[4]. Similarly, a Pu atom in isolation is expected to have a local moment arising from the incomplete 5f shell, and one way to approximate this is to dissolve small quantities of Pu in a non magnetic lattice such as Pd. Instead of forming the simple local moments of a Kondo impurity as was observed for dilute Np in Pd, Pu acts like a local spin fluctuation system with a characteristic temperature, $T_{sf} \sim 1$ K and an effective moment of $1\mu_B$ /Pu[5]. Similarly, dilute doping of Pu into La sharply decreases T_c in contrast to doping Am into La which has a minimal impact on T_c [6]. This again implies a magnetic state for the Pu atoms when individual atoms are isolated within a non-magnetic lattice.

The converse of the above doping experiments would be to remove or displace isolated Pu atoms from a regular

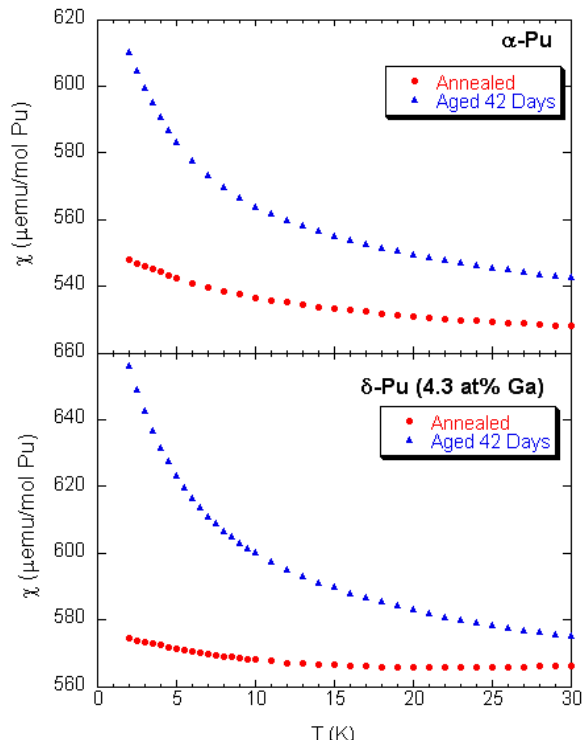


Fig. 1 Magnetic susceptibility taken at 3T

lattice, effectively doping with vacancies and/or interstitials, and observe what, if any, influence this has on the magnetic properties. Pu decays by emission of a 5 MeV alpha particle with a corresponding 86 keV U recoil, generating a damage cascade of ~2500 vacancies and interstitials. Most of these immediately recombine, but a few hundred defects remain, and at sufficiently low temperatures ($T < 35\text{K}$), they become frozen within the lattice. In other words, at low temperatures Pu dopes itself with vacancies (and interstitials). This damage is observable as an increase in the magnetic susceptibility with time (damage) that returns to the undamaged initial ($t=0$) value after annealing to 350K and consistent with earlier resistivity measurements [7]. Thus the excess magnetic susceptibility (EMS) arises from the defects, and not the decay products which are unaffected by thermal annealing. The EMS is strongly temperature dependant, as shown in Fig. 1 for annealed and representative 42-day damaged curves, thereby suggesting there are evolving localized spins and hinting at characteristics of the 5f electrons hidden in the undamaged material.

This work was performed under the auspices of the U.S. Department of Energy by University of California, Lawrence Livermore National Laboratory under Contract W-7405-Eng-48.

- [1] P. Soderlind, and B. Sadigh, Phys. Rev. Lett. **92**, 185702 (2004).
- [2] J. C. Lashley *et al.*, Phys. Rev. B **72**, 054416 (2005).
- [3] H. H. Hill, in Plutonium 1970 and Other Actinides, edited by W. N. Miner (Metall.Soc. and Amer. Inst. Mining, 1970), p. 2.
- [4] A. T. Aldred *et al.*, Phys. Rev. B **19**, 300 (1979).
- [5] M. B. Brodsky, Rep. Prog. Phys. **41**, 1547 (1978).
- [6] H. H. Hill *et al.*, Physica **55**, 615 (1971).
- [7] M. J. Fluss, *et al.*, J. Alloys Compd. **368**, 62 (2004).

Oxidation and aging in U and Pu probed by spin-orbit sum rule analysis: Indications for covalent metal-oxide bonds

K. T. Moore^{1*}, G. van der Laan², R. G. Haire³, M. A. Wall¹, and A. J. Schwartz¹

1. Lawrence Livermore National Laboratory, Livermore, California 94550, USA
2. Magnetic Spectroscopy Group, Daresbury Laboratory, Warrington, UK
3. Oak Ridge National Laboratory, MS-6375, Oak Ridge, Tenn 37831, USA

Transmission electron microscopy is used to acquire electron energy-loss spectra from phase-specific regions of Pu and U metal, PuO₂ and UO₂, and aged, self-irradiated Pu metal. The N_{4,5} (4d to 5f) spectra are analyzed using the spin-orbit sum rule. Our results show that the technique is sensitive enough to detect changes in the branching ratio of the white-line peaks between the metal and dioxide of both U and Pu. There is a small change in the branching ratio between different Pu metals, and the data trends as would be expected for varying f electron localization, i.e., alpha-Pu, delta-Pu, and aged delta-Pu. Moreover, our results suggest that the metal-oxide bonds in UO₂ and PuO₂ are strongly covalent in nature and do not exhibit an integer valence change as would be expected from purely ionic bonding.

High Pressure, High Strain Rate Laser Materials Science

B. Remington- LLNL

Determining the Electronic Structure of Pu using Unorthodox Spectroscopies

James G. Tobin

Lawrence Livermore National Laboratory, Livermore, CA, USA

Email: Tobin1@LLNL.Gov

The standard method to determine the band structure of a condensed phase material is to (1) obtain a single crystal with a well defined surface and (2) map the bands with angle resolved photoelectron spectroscopy (occupied or valence bands) and inverse photoelectron spectroscopy (unoccupied or conduction bands). Unfortunately, in the case of Pu, the single crystals of Pu are either nonexistent, very small and/or having poorly defined surfaces. Furthermore, effects such as electron correlation and a large spin-orbit splitting in the 5f states have further complicated the situation. Thus, we have embarked upon the utilization of unorthodox electron spectroscopies, to circumvent the problems caused by the absence of large single crystals of Pu with well-defined surfaces. The talk will include a discussion of resonant photoelectron spectroscopy [1], x-ray absorption spectroscopy [1,2,3,4], electron energy loss spectroscopy [2,3,4], Fano Effect measurements [5], and bremsstrahlung isochromat spectroscopy [6], including the utilization of micro-focused beams to probe single-crystallite regions of polycrystalline Pu samples. [2,3,6] This work was performed under the auspices of the U.S. DOE by Univ. of California, Lawrence Livermore National Laboratory under contract W-7405-Eng-48.

1. J.G. Tobin, B.W. Chung, R. K. Schulze, J. Terry, J. D. Farr, D. K. Shuh, K. Heinzelman, E. Rotenberg, G.D. Waddill, and G. Van der Laan, "Resonant Photoemission in f-electron Systems: Pu and Gd", *Phys. Rev. B* **68**, 155109 (October 2003).
2. K.T. Moore, M.A. Wall, A.J. Schwartz, B.W. Chung, D.K. Shuh, R.K. Schulze, and J.G. Tobin, "The Failure of Russell-Saunders Coupling in the 5f States of Plutonium", *Phys. Rev. Lett.* **90**, 196404 (May 2003).
3. G. van der Laan, K.T. Moore, J.G. Tobin, B.W. Chung, M.A. Wall, and A.J. Schwartz, "Applicability of the spin-orbit sum rule for the actinide 5f states," *Phys. Rev. Lett.* **93**, 097401 (Aug 2004).
4. J.G. Tobin, K.T. Moore, B.W. Chung, M.A. Wall, A.J. Schwartz, G. van der Laan, and A.L. Kutepov, "Competition Between Delocalization and Spin-Orbit Splitting in the Actinide 5f States," *Phys. Rev. B* **71**, 085109 (2005).
5. S.W. Yu, T. Komesu, B.W. Chung, G.D. Waddill, S.A. Morton, and J.G. Tobin, "f-electron correlations in nonmagnetic Ce studied by means of spin-resolved resonant photoemission," *Phys. Rev. B* **73**, 075116 (2006); J.G. Tobin, S.A. Morton, B.W. Chung, S.W. Yu and G.D. Waddill, "Spin-Resolved Electronic Structure Studies of Non-Magnetic Systems: Possible Observation of the Fano Effect in Polycrystal Ce," *Physica B* **378-380**, xxxxx (2006).
6. J.G. Tobin, M.T. Butterfield, N.E. Teslich Jr., R.A. Bliss, M.A. Wall, A.K. McMahan, B.W. Chung, A.J. Schwartz, "Using Nano-focussed Bremsstrahlung Isochromat Spectroscopy (nBIS) to Determine the Unoccupied Electronic Structure of Pu," in "Recent Advances in Actinide Science," The Royal Society of Chemistry, UK, 2006.

Actinide Sample Preparation for Materials Science, Chemistry, and Physics

M. A. Wall, J. J. Welch, A. J. Schwartz, and M. J. Fluss

Lawrence Livermore National Laboratory, Livermore CA 94550 USA

Abstract

The development of the Actinide Sample Preparation Laboratory commenced in 1998 driven by the need to perform transmission electron microscopy studies on aged plutonium alloys. Remodeling and construction of laboratory space in the Chemistry and Materials Science Directorate at LLNL was required to turn a radiological laboratory into a type III workplace. A dry-train glove box (Figure 1) with a baseline atmosphere of 1 ppm oxygen and 1 ppm water vapor was installed to facilitate sample preparation with a minimum of oxidation or corrosion. This glove box continues to be the most crucial element of the laboratory allowing essentially oxide-free sample preparation for LLNL-based characterizations such as transmission electron microscopy, electron energy loss spectroscopy, optical microscopy, electrical resistivity, ion implantation, and differential scanning calorimetry. In addition, the glove box is used to prepare samples for experiments at world-class facilities such as the Advanced Photon Source at Argonne National Laboratory, the European Synchrotron Radiation Facility in Grenoble, France, the Stanford Synchrotron Radiation Facility, the National Synchrotron Light Source at Brookhaven National Laboratory, the Advanced Light Source at Lawrence Berkeley National Laboratory, and the Triumph Accelerator in Canada.

Preparation Methodology

Nearly all of the sample preparation procedures are based upon the fundamental metallographic preparation procedures of dicing, lapping, polishing, etching, and electrochemical polishing¹. The experimental methodology for sample preparation and design is based upon a lowest common denominator shaped sample. Simple put, a standard 3mm diameter transmission electron microscopy (TEM) sample shape is the basic geometry for virtually all of the small scale science experiments. For example, prior to thinning a 3mm diameter by 100 μ m thick TEM disc to electron transparency it is possible to (i) prepare one side of the sample for optical microscopy (figure 2), (ii) perform standard X-ray diffraction, (iii) measure resistivity² (Figure 3), (iv) further thin for EXAFS³ (Figure 4) and/or in-elastic X-ray studies⁴ (Figure 5a,b), (v) finally thin for TEM studies (Figure 6a,b).

Conclusion

The combination of small sample methodologies, adapted conventional sample preparation techniques, and custom built laboratory and glovebox designs has lead to versatile, efficient sample preparation of actinide samples for a wide variety of small-scale experimentation.

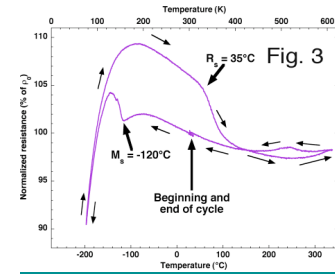
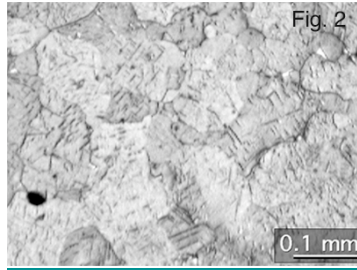
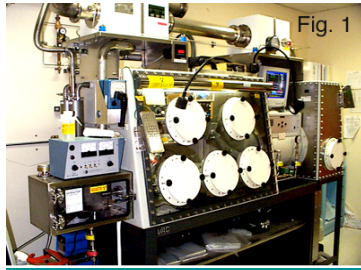


Figure 1. Glove box for small-scale sample preparation. **Figure 2.** Optical micrograph of a delta phase Pu-Ga sample after partial transformation to alpha-prime as a result of quenching to -120°C for ≈ 100 minutes. **Figure 3.** Resistivity data from a cooling and heating cycle of a Pu-Ga “TEM” disc specimen.

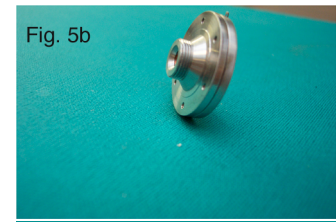
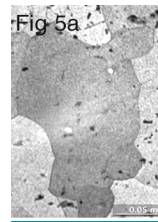
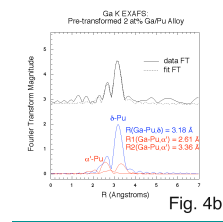
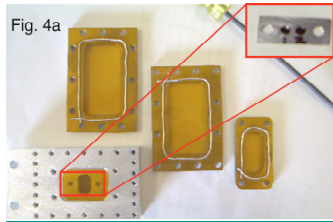
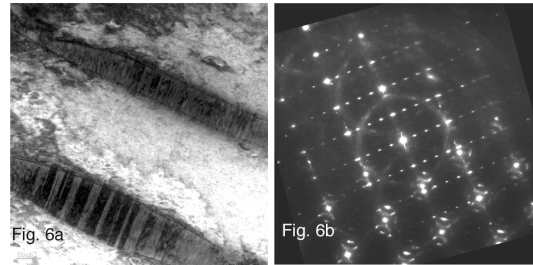


Figure 4.a) Insert shows 2 each, $\approx 10\mu\text{m}$ thin, “TEM” disc specimens that will be sealed inside a double Kapton windowed holder for EXAFS experiments. **b)** EXAFS data from a two-phase delta-alpha Pu-Ga sample. **Figure 5.a)** Optical micrograph of a large grain grown by stain-annealing for in-elastic X-ray experiments that produced the first measurements of the FCC Pu phonon dispersion curves. **b)** Double Kapton windowed sample holder for $\approx 8\mu\text{m}$ thick “TEM” disc samples used for the phonon dispersion experiments. **Figure 6 a)** Bright field TEM image of alpha-prime plates in a delta matrix. **b)** Electron diffraction from the alpha-prime plates and the delta matrix showing the Zocco orientation relationship.



This work was performed under the auspices of the U.S. Department of Energy by the University of California Lawrence Livermore National Laboratory under contract No. W-7405-Eng-48.

References:

- 1) Sample Preparation for Transmission Electron Microscopy Characterization of Pu Alloys, M. A. Wall, A. J. Schwartz and M. J. Fluss, LLNL report, # UCRL-ID-141746..
- 2) Phase Transformation Hysteresis in a Plutonium Alloy System, J.J. Haslam, M.A. Wall, D.L. Johnson, D.J. Mayhall, and A.J. Schwartz, MRS Proceedings, 2001, UCRL-JC-144283.
- 3) Local structure and vibrational properties of Alpha-Pu, Alpha-U, and the Alpha charge density wave, E. Nelson, P. Allen, K. Blobaum, M. Wall, C. Booth, *Phy. Rev. B* 71, 184113 (2005).
- 4) Phonon Dispersions of fcc -Plutonium-Gallium by Inelastic X-ray Scattering, Joe Wong , M. Krisch, D. Farber, F. Ocelli, A. Schwartz, T.C. Chiang, M. Wall, C. Boro and Ruqing Xu, *Science*, 301, 1078 (2003).

New opportunities for high-pressure materials research at the HPCAT at APS

C.S. Yoo-LLNL